Graduate Student Theses, Dissertations, & Professional Papers

Graduate School

2005

Developing a disturbance index and extreme land surface temperature in the western United States

David J. Mildrexler
The University of Montana

Recommended Citation

Mildrexler, David J., "Developing a disturbance index and extreme land surface temperature in the western United States" (2005). *Graduate Student Theses, Dissertations, & Professional Papers*. 8290.
https://scholarworks.umt.edu/etd/8290

Maureen and Mike
MANSFIELD LIBRARY

The University of

Montana

Permission is granted by the author to reproduce this material in its entirety, provided that this material is used for scholarly purposes and is properly cited in published works and reports.

Please check "Yes" or "No" and provide signature

Yes, I grant permission   ___✓___

No, I do not grant permission   _____

Author's Signature: _David Joseph Mildrude_

Date: _May 17, 2005_

Any copying for commercial purposes or financial gain may be undertaken only with the author's explicit consent.

8/98

DEVELOPING A DISTURBANCE INDEX AND EXTREME LAND

SURFACE TEMPERATURE IN THE WESTERN UNITED STATES

by

David Mildrexler

B.Sc. Portland State University, 1999
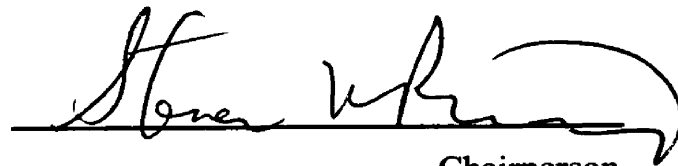
presented in partial fulfillment of the requirements
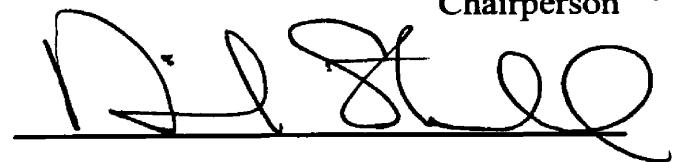
for the degree of

Master of Science

The University of Montana

May 2005

Approved by:

_____
Chairperson

_____
Dean, Graduate School

_____10 May 2005_____
Date

Mildrexler, David J. M.S., May 2005   Forestry and Conservation, Remote Sensing

Developing a Disturbance Index and Extreme Land Surface Temperature in the Western United States

Chairperson: Steven W. Running

   Land surface temperature (LST) is one of the key parameters in the physics of land surface processes, combining surface-atmosphere interactions and the energy fluxes between the atmosphere and the ground. Increases in LST could produce profound changes in the forests at high and temperate latitudes, and result in increased carbon dioxide emissions from terrestrial disturbance events such as drought and wildfire. The timing, location and magnitude of major disturbance events is currently a major uncertainty in the global carbon cycle. The Aqua sensor, aboard the Terra Spacecraft, was launched in 2002 and has yet to be tested for its full capacity as a land surface remote sensor. The MODIS/Aqua 11 LST product provides global estimates of radiometric LST with continuous spatial coverage. We analyze the sensitivity of the LST estimates at the fine scale by comparing the maximum LST of a poplar tree plantation in the desert of eastern Oregon to the adjacent natural land cover types. At the coarse scale, a strong negative correlation was observed between the mean-maximum LST and the mean-maximum enhanced vegetation index (EVI) over all biomes in the western United States. Based on this relationship we develop a disturbance index using LST and the EVI. Our results indicate that the LST/EVI interannual disturbance index is capable of detecting relatively large disturbances with good accuracy, such as wildfire, and the impacts of interannual weather variability on vegetation. LST maps highlighting physiologically defined potentially lethal LST were created and compared to biome distribution. The extreme temperature maps provide a fresh look into the spatial distribution and interannual variability of these temperatures.

Acknowledgements

Thanks to my committee for all the enthusiastic support, ideas, and suggestions that have been vital in shaping the direction of this project. A special thanks to Dr. Maosheng Zhao, whose expertise has been instrumental in the progress of this work and to Dr. Faith Ann Heinsch, for her steady help and unique skill of remembering what it is like to be in someone else's shoes. Thanks to the entire Numerical Terradynamic Simulation Group (NTSG), an awesome group that has always been willing to help the "fish out of water" I have sometimes felt myself to be. For me, the most important part of the NTSG has certainly been the "G".

I wish to extend my deepest gratitude to my fiancée, Annie for her constant support and encouragement. To my family, for the constant awareness that I have of you being with me. In other words, "no windows, but plenty of the love." To my cousin Paul, and my dear friends Brit, and Lucrecia, may you be at deep peace.

Table of Contents

List of Tables

List of Figures

List of Appendices

Introduction

Landscape-level spatial data of disturbance location and intensity on the Earth surface is important for tracking responses of the biosphere to climate change, for global carbon budget modeling, and for improved resource management. An ecological disturbance is an event that results in a sustained disruption of ecosystem structure and function (Picket and White, 1985; Tilman, 1985). Many of these events alter ecosystem productivity and resource availability (light and nutrients) for organisms on large spatial and temporal scales (Potter et al., 2003). Ecosystem scientists have yet to develop a proven methodology to monitor and understand major disturbance events and their historical regimes at a global scale (Potter et al., 2003). The ability to monitor disturbance and track the recovery of disturbed areas is critical to understanding the response of the biosphere to a constantly changing climate.

In the past, vegetation has responded to warming and temperatures that were higher than are current temperatures. However, the novelty of the expected changes in the 21st century is the rate of increase in temperature (Flenley, 1998). A range of credible scenarios of greenhouse gas emissions could increase radiative forcing, leading to a 3-6°C increase in mean near-surface air temperature at high and temperate latitudes during this century (Houghton et al., 1996; Kattenburg et al., 1996). Such increases could result in profound changes in the forests of North America (Shriner and Street, 1998) as the geographical ranges of many tree species are predicted to shift northward (Davis and Zabinski, 1992; Dyer, 1995; Iverson et al., 1999). Insect herbivores of tree species will also shift ranges to follow their hosts (Williams and Liebhold, 1997). Early results have suggested that rates of change exceeding the ability of ecosystems to migrate would be

particularly damaging (McCarthy et al., 2001). As climate change accelerates, disturbance processes could play an increasingly important role in land cover change. Shifts in land cover distribution could greatly alter our natural resource dependent socio-economic opportunities, influence the suitability of large areas for agricultural use, alter our development patterns, and have drastic effects on native plant and animal species.

Increases in temperature will be inextricably linked to increases in carbon dioxide (CO_2), vapor pressure deficit (VPD), drought, and in some regions, fire frequency (Saxe et al., 2001). Because major 'pulses' of CO_2 from terrestrial biomass loss can be emitted to the atmosphere during large disturbance events, the timing, location, and magnitude of vegetation disturbance is presently a major uncertainty in understanding the global carbon cycle (Canadell et al., 2000). Elevated biogenic sources of CO_2 have global implications for climatic change, which can in turn affect a vast number of species on Earth and the functioning of virtually all ecosystems (Potter et al., 2003). An improved and automated disturbance metric for continental change detection is urgently needed and if the effects of those disturbances could be quantified, could serve as a key input into carbon budget models.

The responses of plants to the severity of their environment have occupied the attention of man long before the beginnings of the science of biology (Levitt, 1941). The dependence of humans on vegetation for oxygenation of the atmosphere, food, fiber, and medicine has driven both a curiosity and a need to explore the limits and tolerances of plant communities. The physiological consequences of extreme temperature exposure on plant growth, reproduction, and survival have been thoroughly examined (Larcher, 2003; Levitt, 1980; Turner and Kramer, 1980). However, accurately mapping the occurrence of

2

extreme or potentially lethal temperatures instantaneously and continuously across the land surface has, until now, not been feasible. Maps of potentially lethal land surface temperature based on spatially contiguous remotely sensed data offer new opportunities to explore stress physiology concepts that have been heretofore limited to laboratory and small plot-based experiments, at a landscape level. This, in turn, could lead to a greater ability of researchers to communicate findings with land managers. Physiologically defined potentially lethal temperature maps could be used to assess human health hazards such as the potential for the spread of pathogens and viruses, the suitability of areas as wildlife habitat based on seasonal extreme temperatures, or the influence of agricultural development on lethal temperature patterns.

Aqua/MODIS Land Surface Temperature

Land surface temperature (LST) is one of the key parameters in the physics of land surface processes on regional and global scales (Wan et al. 2004), combining surface-atmosphere interactions and the energy fluxes between the atmosphere and the ground (Mannstein, 1987; Sellers et al., 1988). Interactions between the land surface and the atmosphere and the resulting exchanges of energy and water have a large impact on climate (Shukla and Mintz, 1982). LST is an important factor in modeling large-scale hydrological systems, global primary production, the effect of greenhouse gases, and in a wide variety of ecological and biogeochemical studies (Running et al., 1994). The MODIS LST products are key inputs to many of the higher-level MODIS products and provide data for global temperature mapping and change observation.

The Aqua/MODIS LST product is provided as global, pixel-wise estimates of radiometric land surface temperature at 1-km^2, 5-km^2 and .05° resolutions. Radiometric temperature measures the radiation that is emitted by a body from some distance, in this case by satellite. LST is defined as the radiation emitted by the top of the land surface observed by MODIS at instantaneous viewing angles. "Land surface" refers to canopy in vegetated areas or soil surface in bare areas (Wan et al., 2004).

The Aqua/MODIS instrument

As part of the Earth Observing System, the second of two MODIS instruments was launched on May 4th, 2002. The MODIS instrument on-board the Aqua platform is used to measure LST, vegetation dynamics, and land cover and land use change as well as other ecological parameters. The first full year of data collected from the MODIS/Aqua sensor was 2003. The strengths of the MODIS instrument include its global coverage, high radiometric resolution and dynamic ranges, and accurate calibration in the visible, near-infrared and thermal infrared (TIR) bands (Wan et al., 2004). The MODIS instrument has 36 bands with bands 1-19 and band 26 in the visible and near infrared range, and the remainder of the bands in the thermal range from 3 to 15 μm (Wan, 1999). The LST of clear-sky pixels in MODIS scenes is retrieved from brightness temperatures in bands 31 and 32 with the generalized split-window algorithm (Wan and Dozier, 1996). The MODIS LST bands based on TIR data are only available under clear sky conditions because clouds inhibit satellite observations in the visible and TIR spectral ranges. Cloud contamination limits availability of good quality TIR based

4

LST data with a temporal and spatial bias due to the effects of seasonality and topography on cloud formation.

The Aqua/MODIS sensor was chosen for this study because of its afternoon equatorial crossing time. Terra's orbit around the Earth is timed so that it passes from north to south across the equator around 10:30 am, while Aqua passes south to north over the equator around 1:30 pm (Wan et al., 2004). Because of the Aqua overpass time around 1:30 pm, the afternoon LSTs retrieved from the Aqua/MODIS data will be closer to the peak of diurnal fluctuation and to the maximum temperature of the land surface. As a result, it is more suitable for regional and global change studies (Wan et al., 2004). The partitioning of sensible and latent heat at the vegetated land surface is critical for determining both photosynthetic activity and LST. Morning measurements will typically be lower than afternoon measurements due to the potential for morning dew, higher vapor pressure and less solar radiation loading. As the daytime temperature and VPD rise, the amount of energy partitioned as sensible heat flux increases at the vegetated surface resulting in higher surface temperatures. Measurements close to the peak of diurnal fluctuation will better reflect the thermal response of rising leaf temperatures due to decreased latent heat flux as stomata close to minimize water loss by transpiration, and the occurrence of potentially lethal temperatures.

LST Algorithm Theoretical Basis

One of the major difficulties in development of LST algorithms is the considerable spectral variation in emissivities for different land-surface materials. Emissivity may also vary with the satellite viewing angle (Dozier and Warren, 1982;

Labed and Stoll, 1991; Rees and James, 1992), an effect that is more important over land than water because the combination of surface slope and MODIS scan angle routinely results in local viewing angles greater than 60° and pixel distortion. It is essential to measure spectral emissivities of natural cover types for the development of LST algorithms. Strategy for development of the MODIS LST algorithms consisted of: 1) the establishment of a comprehensive land surface emissivity and BRDF (Bidirectional Reflectance Distribution Function) knowledge-base in a joint effort with the EOS ASTER Science Team so that the development of the MODIS LST algorithms has a solid basis and so that it is possible to measure LST with an accuracy better than 1 K for ground-based validation of the product; 2) the use of accurate radiative transfer models that incorporate new theoretical and experimental advances in atmospheric absorption into simulations; and 3) the establishment of a database from accurate radiative transfer simulations and development of a look-up table and interpolation scheme so that efficient and accurate physics-based LST algorithms for retrieving surface emissivity and temperature could be used in operational production (Wan, 1999).

Quality control

Automatic quality control is performed on a routine basis at the Distributed Active Archive Center (DAAC). Quality flags are provided for each LST pixel so that a quality control image corresponds to a LST image. The quality flag is an 8-bit code indicating the confidence in LST processing. More details can be found in the MODIS Land-Surface Temperature Algorithm Theoretical Basis Document, Version 3.3 (Wan, 1999).

Assumptions

The MODIS LST algorithm, as well as most existing LST algorithms, is based on the simple assumption that a land surface pixel can be described by different spectral emissivities and a single effective radiometric temperature in all TIR bands. But this may not be true for pixels containing sub-pixel fires. Snow-surface temperature retrieval is very difficult, if not impossible, because snow emissivity varies with depth, density, and grain size. Land surfaces with large areas of water present, such as lakes and flooded soils, also present problems because of the integrated influence of the much lower brightness temperatures and higher polarization differences for water (McFarland et al., 1990). When linking pixel values to fixed coordinates on the Earth's surface, the MODIS LST, as well as all other land products, will have troubles with complicated mixed pixels along land cover boundaries in terms of their quantitative definitions, quality assessments and applications (Wan, 1999).

Algorithm validation and uncertainties

Prelaunch validation is a comparison between temperatures retrieved from in-situ measurements and those retrieved from airborne and satellite TIR data. The LST product is considered valid when the measurements and error analysis indicate an absolute accuracy of the aerial or satellite measurements of better than 1 K standard deviation (Wan, 1999). The uncertainty in LST retrieved by the generalized split-window LST algorithm for uniform land surfaces with known spectral emissivity characteristics could be equal to or smaller than 0.5 K (Li and Becker, 1993; Wan and Dozier, 1989). Uncertainty is more difficult to assess for pixels at the maximum scanning angle (+ or -

55°), for which local viewing zenith angle is approximately 65° resulting in pixel distortion. This difficulty has been overcome through the following improvements; 1) viewing angle is considered in the algorithm; and 2) the LST algorithm is optimized over atmospheric column water vapor and temperature ranges (Wan, 1999).

Dimensions of LST variability

Over land surfaces, temperatures derived from satellite data are a complex function of:

1) surface properties (canopy cover and density, emissivity, fractions of sunlit and shaded areas in the pixel, moisture status);

2) atmospheric conditions (solar radiation, vapor pressure, wind speed, advection); and,

3) viewing geometry of the sensor.

In mountainous terrain, topography plays a dominant role influencing LST through changes in solar radiation loading (south-facing versus north-facing slopes), and atmospheric lapse rates (Nemani et al., 1993). Seasonality is also a significant source of LST variability.

Each land cover type has distinct interactions with the atmosphere that can result in different local meteorological conditions. This reciprocal influence of vegetation on the microclimate of the particular area results from vegetation properties such as aerodynamic roughness, leaf seasonality, leaf area index, and partitioning of sensible and latent heat fluxes at the vegetation or ground surface. Goward et al. (1985) suggest the possibility of using the rate of change in surface temperature with the amount of

8

vegetation to describe surface characteristics. The underlying principle for such a technique is that surface temperature decreases with an increase in vegetation density through latent heat transfer, though the decrease in surface temperature is modulated by the synoptic state of the atmosphere as well as the aerodynamic and canopy resistances operating at the surface (Nemani and Running, 1988). Nemani and Running (Figure 1; 1997) developed a conceptual diagram that illustrates the dynamics of the surface temperature (T_s)-Normalized Difference Vegetation Index (NDVI) relationship for various vegetation types. The T_s-NDVI space is divided into four simple groups chosen to represent energy absorption and exchange characteristics of various land cover types.
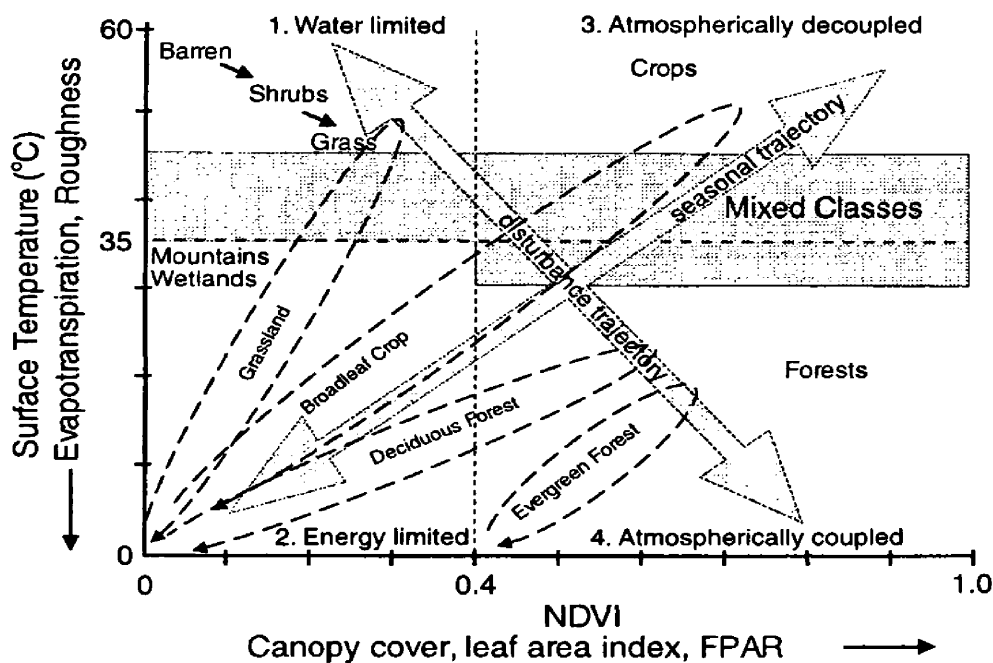
Figure 1. Dynamics of T_s-NDVI for various vegetation types where seasonal trajectories indicate phenological evolution of vegetation and the disturbance trajectory is useful for change detection over time (Nemani and Running, 1997).

When land covers are stratified within the Ts-NDVI space, an energy balance results, where decreasing LST is coupled with increasing vegetation density. Disturbance causes shifts in the energy balance relationship and movement along the disturbance trajectory.

Goetz (1997) reported that the negative correlation between LST and NDVI, observed at several scales (25 m^2 to 1.2 km^2), was largely due to changes in vegetation cover and soil moisture, and indicated that the surface temperature can rise rapidly with water stress. Keeping in mind that from a remote sensor, the land surface for closed canopy forests would be the top surface of the canopy, we expect that for dry conditions, areas with high vegetation density will show a stronger resistance to a change in surface temperature due to greater partitioning of energy as latent heat. Patches with low vegetation density should show little resistance to surface temperature changes due to greater partitioning of solar radiation as sensible heat. Disturbance resulting in decreased vegetation density should see an increase in LST as sensible heat flux increases.

Monitoring LST may amplify our ability to track disturbance and recovery on the land surface. Leafy vegetation cover is likely the most fragile and therefore perhaps the single most vulnerable biotic component of terrestrial ecosystems to detectable alteration during disturbance events (Potter et al., 2003). Disturbances such as wildfire, urban development, and irrigation result in conditions that alter vegetation and, therefore, the energy balance of a site. Tracking interannual (pre and post-disturbance) LST may provide a method for quantifying disturbance at the landscape level and can be used to improve models and methods for evaluating land-surface energy balance (Crag et al., 1995; Diak and Whipple, 1993). The magnitude of the LST response to disturbance should in part be dependent on the pre-disturbance vegetation density and on the disturbance intensity as related to alteration of the vegetation.

Stress physiology

It has long been known that temperature is one of the critical environmental stresses to which an organism may be subjected. Defining critical temperature thresholds quantitatively is very difficult due to the variation in stress tolerance and stress resistance strategies among species. Evergreen needle leaf forest has adapted to freezing surface temperatures but seldom reaches lethally high LST. By contrast, ability to cope with high temperature is an important factor in determining the success and distribution of plants in hot, arid habitats (Turner and Kramer, 1980). As climate change increases LST, the ability of biomes to cope and adapt to extreme high temperature could become an increasingly important factor for land cover distribution.

Plants regulate their temperature by dissipating part of the energy they absorb and thus preventing injury or death due to excessively high temperature. Of the three major mechanisms (reradiation, transpiration, and convection), reradiation dissipates one-half of the energy that plants absorb (Gates, 1980). Transpirational cooling accounts for an additional heat loss when energy is expended changing water into water vapor. In addition, convection across the thin air zone that surrounds all surfaces in still air (i.e., the boundary layer) acts to transfer heat from the leaf to cooler air.

High temperature

Plant processes function across a broad range of tissue temperatures, generally 0°C to 50°C, as long as living cells and their proteins are stable and enzymatically active (Barnes et al., 1998). As temperature increases, plant activities increase up to an optimum temperature and then decrease until, at very high temperatures, enzymes and

structural proteins are inactivated or denatured, and death occurs. As temperature rises, the conformational entropy favoring the denatured state increases more rapidly than the increase in strength of the hydrophobic bonds, and a temperature is finally reached at which unfolding of proteins begins (Levitt, 1980). The heat-killing temperature for some thirty-nine species of plants from August to September on the coast of Spain ranged from 44°C to 55°C (Lange and Lange, 1963). Temperate zone evergreen conifers have a temperature threshold for heat injury during the growth season of 44°C to 52°C (Larcher, 2003) and a number of studies with various tree species (Baker, 1929; Barnes et al., 1998; Lorenz, 1939) seem to indicate that the lethal point occurs at about 55°C.

In contrast to the relatively minor role of exposure time in the case of freezing, the time subjected to high temperatures is of fundamental importance. This is true not only of vegetative plants but also of seeds, which can be killed within seconds to minutes by heat shocks of 60°C to 120°C (Levitt, 1980). Not only does the heat-killing temperature vary inversely with the exposure time, but the relationship to time is actually exponential.

The greatest danger of heat injury occurs when the soil is exposed to insolation, reaching temperatures as high as 55°C to 75°C (Lundegardh, 1949). One of the most serious seedling "diseases," according to Munch (1913) is the killing of a narrow strip of bark around the stem of young woody plants at soil level when soil temperatures exceed 46°C. Since temperatures above 50°C are largely confined to the exposed ground-air boundary in forests, direct heat injury to forest trees is most significant in its effect on small seedlings, which have relatively unprotected live tissues in this critical zone (Baker, 1929; Barnes et al., 1998). Surface soil temperatures of 54°C to 71°C have been detected in temperate climates and injury may begin at as low as 49°C (Baker, 1929).

Project goal and objectives

The goals of this study are to develop and test a disturbance index that exploits the ability of the Aqua/MODIS LST data to track land surface disturbance based on changes in energy partitioning and to identify where physiologically defined extreme land surface temperatures occur in the western United States. The main objectives are to:

1. Generate extreme land surface temperature maps of the western United States and interpret the major bioclimatic patterns.

2. Assess the accuracy and sensitivity of the disturbance index based on independent data sources.

Methods

Study area

This study domain for this project is the western United States extending from the Pacific Coast to east of the Rocky Mountains (Figure 2). A broad range of bioclimatic regions are encompassed by the study area, from rainforest in the Pacific Northwest to vast deserts in the Southwest. The north part of the study area transitions from rainforest to high desert across a relatively short west-east distance due to the steep climatic gradient resulting from orographic lifting of warm Pacific air over the Cascade Mountains.

Land Cover Class
- water (water)
- evergreen needleleaf forest (enf)
- evergreen broadleaf forest (ebf)
- deciduous needleleaf forest (dnf)
- deciduous broadleaf forest (dbf)
- mixed forests (mf)
- closed shrubland (cs)
- open shrubland (os)
- woody savannas (wsav)
- savannas (sav)
- grasslands (g)
- permanent wetlands (pwet)
- croplands (crop)
- urban and built-up (urb)
- cropland/natural vegetation mosaic (crop/nat
- snow and ice (snow/ice)
- barren or sparsely vegetated (barren)

Figure 2. The western United States study area extends from the U.S. - Canada Border to the U.S.- Mexico Border and from the Pacific Coast to east of the Rocky Mountains (MODIS tiles h08v04, h08v05, h09v04, h09v05, and h10v04).

MODIS data acquisition and processing

The 8-day composite, 1-km Aqua/MODIS daytime LST (MYD11A2)

Hierarchical Data Format-Earth Observing System (HDF-EOS) blocks for 2003 and 2004

were acquired for the western United States. The 16-day composite, 1-km MODIS

Enhanced Vegetation Index (EVI; MOD13A2) HDF-EOS blocks for 2003 and 2004 were

acquired for the western United States. The western United States is covered by MODIS

tiles h08v04, h08v05, h09v04, h09v05, and h10v04 (Figure 2). The MODIS Land Cover

data (MOD12Q1) were acquired for the year 2003. These data can be ordered from the

Distributed Active Archive Center at http://edcimswww.cr.usgs.gov/pub/imswelcome/.

MODIS quality control was applied to the LST and EVI data. The MODIS cloud mask

for the MOD11A1 Daily LST Product Quality Assurance field was applied to the LST

data (MODIS Science Team: LST-Group, 2003). The MODIS cloud mask for the

MOD13A2 Daily EVI Product Quality Assurance field was applied to the EVI data

(MODIS Science Team: TBRS Lab, 2003). Pixels that were contaminated by

unfavorable conditions such as cloud cover for less than 30% of the eight-day images

during a one-year period were filled based on temporal linear interpolation. Pixels with

greater than 30% contamination were discarded. All HDF-EOS data were converted to

floating point files and then to raster images.

The MODIS Land_Cover_Type_1 (IGBP) was used to assign pixels to a land

cover type. This provided an accurate grouping method so that analyzing complicated

mixed pixels along land cover boundaries was greatly simplified. Grouping pixels based

on land cover provided the means to statistically compare disturbance index results and

lethal temperature results based on land cover type and to explore energy balance relationships across the study area.

This study supplements the first order topographic information in the LST algorithm with a high quality digital elevation model (DEM) at 1 km resolution (http://edcdaac.usgs.gov/order.asp). The DEM was useful for exploring the effects of elevation on lethal temperature patterns and for interpreting the disturbance index results.

Potentially lethal temperature maps

The potentially lethal temperature for this study is defined as any pixel that reaches 50°C or higher. The highest temperature recorded at every pixel during any eight-day period over an annual period (2003 and 2004) was extracted and combined into one image. Pixels with LST of 50°C or higher were highlighted and grouped by 2.5 degree increments. Pixels with LST less than 50°C were mapped on a blue scale and grouped by 5.0 degree increments (Figure 3). A biogeographical approach was taken to analyze the extreme high LST maps where patterns are contrasted with the IGBP land cover map in order to highlight land cover driven extreme temperature variation.

Poplar farm maximum LST sensitivity analysis

The sensitivity of the maximum LST estimates is explored by analyzing the LST of a poplar tree farm in eastern Oregon (45.8° N and 119.5° W) as compared to the natural vegetation adjacent to the tree farm. ASTER imagery at 15 m resolution was used to confirm the location of the tree farm and to compare with the MODIS land cover classification product. Three five-pixel transects were established within the poplar tree

farm, classified as deciduous broadleaf forest, and within the adjacent native plant communities, classified as open shrublands and grasslands. The maximum LST during 2003 and 2004 was extracted for all five pixels at each transect totaling fifteen pixels. The pixels were averaged and the means were compared to test for significant differences in LST among the three groups using three paired two-sided t-tests. A Bonferroni correction was applied, and data were considered statistically significant when p ≤0.03.

Mean-maximum LST and mean-maximum EVI relationship

Mean-maximum LST is calculated as the sum of the highest temperature at each pixel during an annual period within a given land cover type divided by the number of pixels within that land cover type. The mean-maximum value is calculated for each land cover type. The mean-maximum EVI is computed in a similar manner. The land cover stratified mean-maximum LST and the mean-maximum EVI data were tested for normality. Pearson's correlation analysis (r) was used when the data were normal, and the confidence limits (CL) surrounding r were calculated as

$$CL = \sqrt{\frac{1-r^2}{n-2}} \times t_{\frac{\alpha}{2},df} \tag{1}$$

where *n* is the number of samples used in the analysis and t is the Student t-statistic.

A linear regression between the calculated mean-maximum LST and mean-maximum EVI for each land cover type was performed to test the significance of the relationship between EVI and LST.

17

Disturbance Index development

An algorithm was developed to identify significant interannual changes in the annual LST/EVI ratio in order to detect land surface disturbance. The maximum day LST at each pixel during an annual period was divided by the maximum EVI value for each pixel during the same year resulting in an LST/EVI ratio. Prior to this division, all EVI values less than 0.025 were reclassified as no data in the 2003 and 2004 maximum EVI images. These values were mainly associated with water bodies and snow/ice and indicate areas with no vegetation. Extremely low EVI values cause problems in calculation of the index because maximum EVI is the denominator for the annual calculation (Eqn. 2) and order of magnitude differences exist between maximum EVI values on an interannual basis for a given pixel. For example, a pixel within the study area had a maximum EVI value of 0.0491 in 2003 and -0.0002 in 2004. Pixels that have good quality data for only one of the two years are classified as no data. The 2004 LST/EVI ratio was divided by the 2003 LST/EVI ratio on a pixel-by-pixel basis as follows:

$$LST \ / \ EVI \ disturbance \ index \ = \ \frac{\dfrac{Max \ LST \ 2004}{Max \ EVI \ 2004}}{\dfrac{Max \ LST \ 2003}{Max \ EVI \ 2003}} \qquad (2)$$

This results in a ratio of interannual variability computed at each pixel in the study area. The logic used here is that disturbance will result in change to the LST and/or EVI. If no change occurs at a given pixel, the interannual ratio will be near unity. If the land surface has been disturbed, the disturbance index results in a value different than 1.

18

Areas that are recovering from disturbance, as defined by increasing EVI or a decreasing LST, will have values less than 1.

The success of this index depends on two factors; (1) does disturbance generate a large enough LST/EVI signal to detect and (2) is the signal bigger than the natural variability. With only two years of data on an annual basis, a long-term analysis of biome-stratified histograms to determine the threshold that defines disturbance is not possible. Therefore, the mean and standard deviation disturbance index value for the western U.S. was calculated and used as the disturbance threshold for the region. However, disturbance index results were stratified by land cover class and the mean and standard deviation were used to create a biome-stratified scatter-plot. The disturbance index results were verified visually using two fire detection data sets and precipitation anomaly maps. Fire detection data sets include the 2002 and 2003 MODIS active fire detections data (http://activefiremaps.fs.fed.us/fireptdata.php), the Northern Rockies Coordination Group Fire Perimeters for the 2003 fire season (http://www.fs.fed.us/r1/firegis/2003web/dataindex.htm), and the Booth and Bear (B&B) Fire Perimeter Map (http://www.fs.fed.us/r6/centraloregon/fires/2003/b-b/index.shtml). Precipitation anomaly maps for 2003 and 2004 are from the Spatial Climate Analysis Service Prism data collection (http://www.ocs.oregonstate.edu/index.html). Precipitation anomaly maps show precipitation as a percentage of the normal precipitation between 1971 and 2000 at 4 km resolution.

Results

Potentially lethal temperature maps

The lethal temperature maps show the spatial distribution of 50°C and higher temperatures in the western United States for 2003 and 2004 (Figure 3). Mountains generally have maximum LST below 50°C, as seen in the Cascades, Rockies, and Sierra Nevada Mountain Ranges. These mountain ranges are predominantly forested, and forests maintain LST below the lethal temperature threshold. Coastal areas west of the Cascades in Oregon and Washington have maximum LST below 50°C. The maximum LST of the southern Sacramento Valley exceeds 50°C. Interior arid and semi-arid environments (e.g., Great Basin, Mojave and Sonoran deserts) have LST's greater than 50°C for 2003 and 2004.
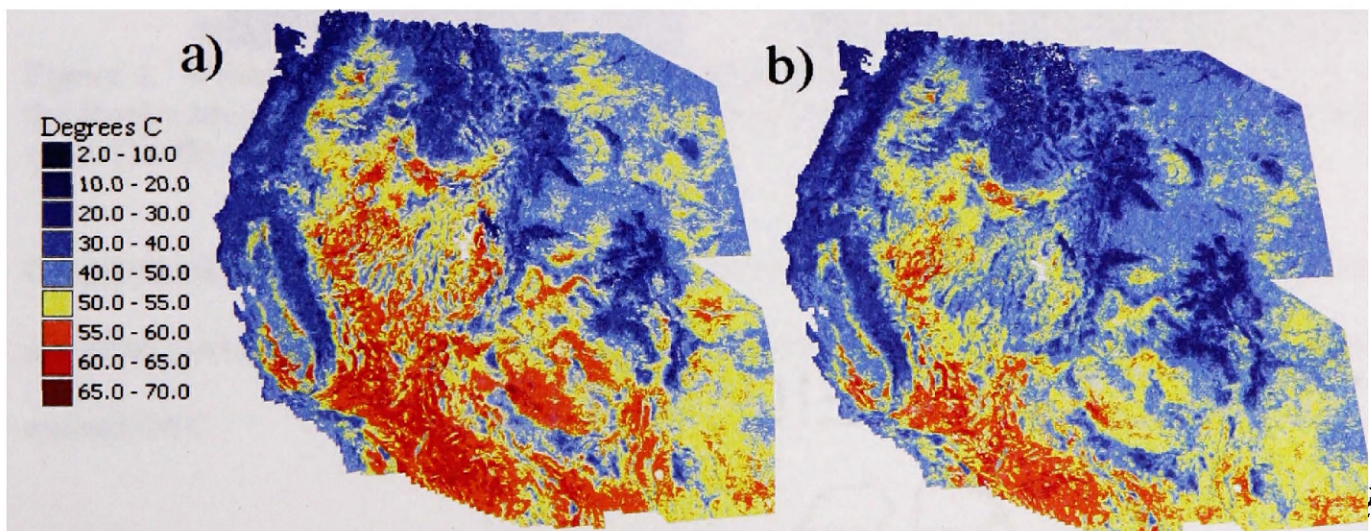
Figure 3. Potentially lethal LST maps for 2003 (a) and 2004 (b) at 1km resolution on a digital elevation model of the western United States.

Lethal temperatures increase in areal extent along a north to south gradient in the western U.S. Interannual variability is high as extreme LST in 2003 has greater areal coverage than extreme LST in 2004. For example, large portions of the northeastern part of the

study area reach the lethal threshold in 2003 and do not in 2004. The central part of the

study area shows the same decline in lethal temperature patterns from 2003 to 2004.

In western Montana, non-forested valleys, such as the Bitterroot Valley (Figure

4b), within an otherwise forested landscape, reach the lethal temperature threshold of

50°C in 2003 and appear as a thin line of pixels (Figure 4a). Grasslands, like those found

west of Polson and east of the Rocky Mountain Front, had LSTs between 50°C and 60°C.
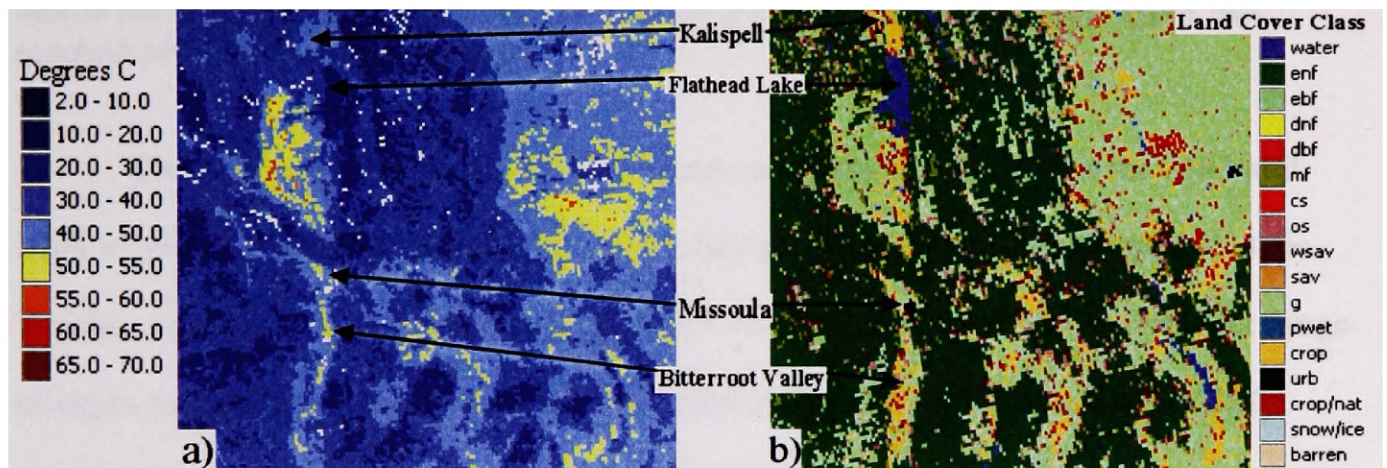
Figure 4. Western Montana 50°C or greater temperatures (a) in the valleys and east of the Rocky Mountain Front coincide with grasslands (b) and other non-forested land cover types (2003).

Croplands (Figure 5a) tend to stay below the lethal temperature threshold (Figure 5b) but

are often surrounded by land cover types (e.g., shrub, savannah, grasslands) that reach or

exceed 50°C.
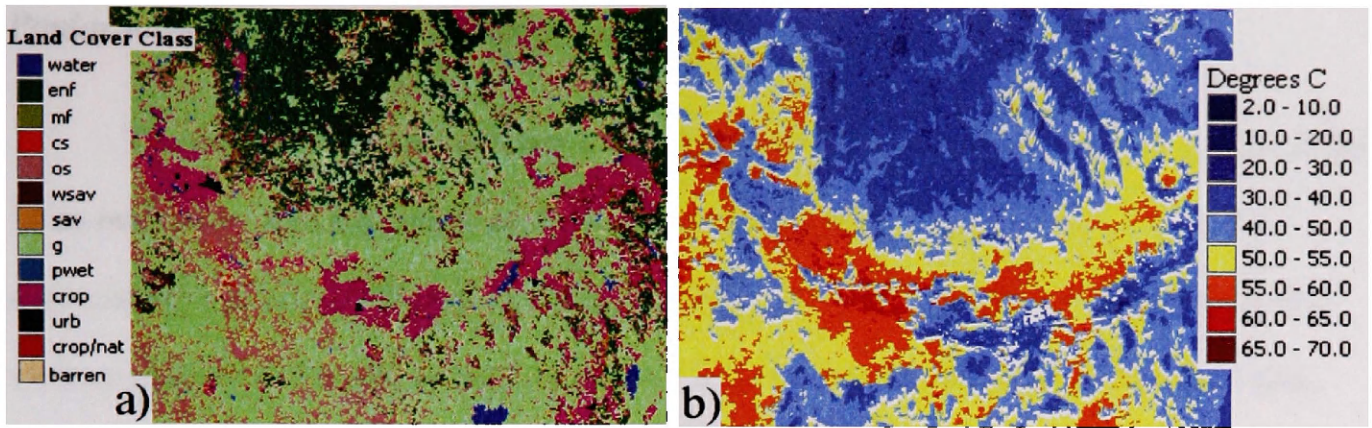
Figure 5. Croplands (highlighted in pink) in Idaho's Snake River Valley (a) have LST below the lethal temperature threshold and are surrounded by land cover types that reached 50°C or greater (b) during 2003.

The timing of acquisition for the maximum daytime LST values for 2003 and 2004 were predominantly between the eight-day periods 153 and 233 (Figure 6), June through August. The frequency of acquisition for 2004 was spread over a broader range of eight-day periods (153 – 233) than it was for 2003 (177 – 233) with 15% of 2004 acquisitions from the consecutive eight-day periods spanning day 153 to 169.
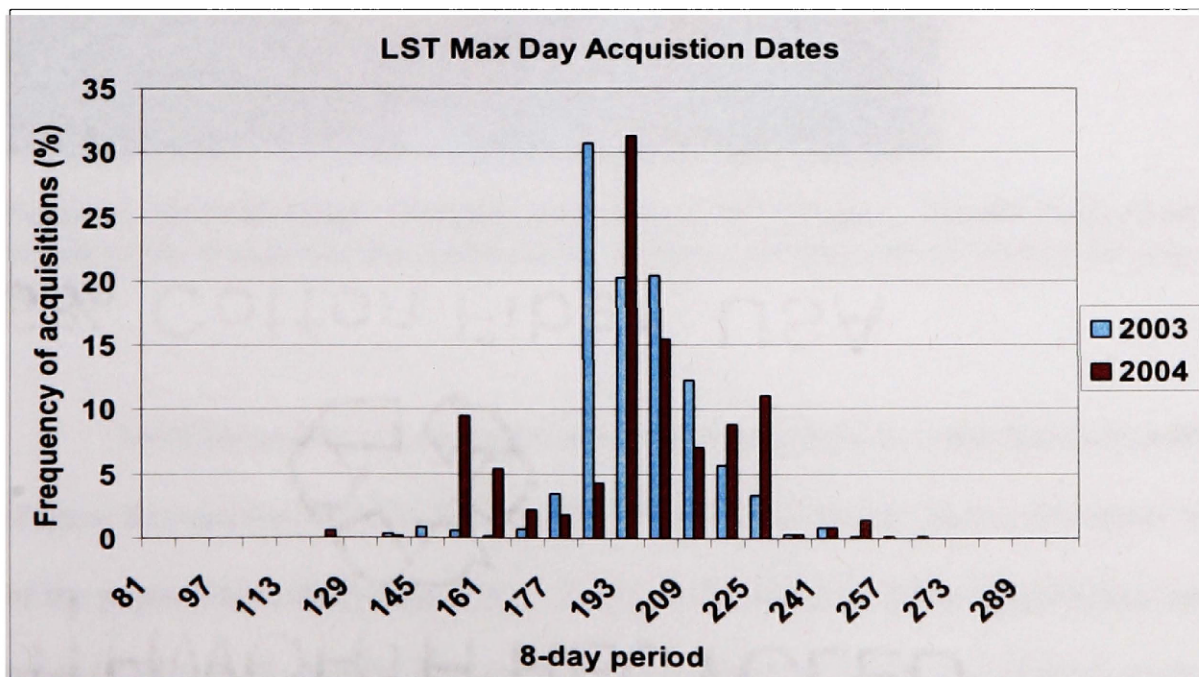
Figure 6. Nearly 100% of maximum LST acquisitions occurred between 8-day periods 153 and 233, approximately June through August for both 2003 and 2004.

The poplar tree farm, located in Northeast Oregon, can be seen in the center of the 15 m resolution ASTER image as the dark red blocks that sharply contrast with the surrounding landscape (Figure 7). The Columbia River bisects the top of the image and various agricultural lands, as well as undeveloped areas, surround the poplar tree farm.
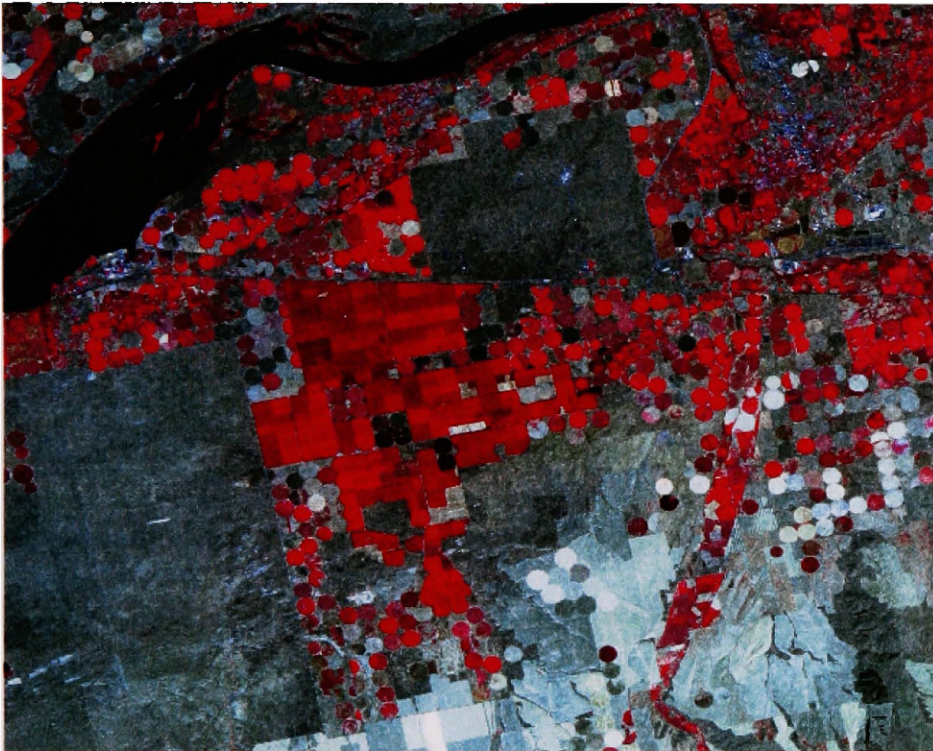
Figure 7. ASTER image of poplar tree farm in NE Oregon. The dark red squares in the center of the image are the poplar farm and the Columbia River bisects the top of the image.

MODIS land cover classifies the poplar tree farm as a deciduous broadleaf forest (Figure 8a) and the MODIS EVI product (Figure 8b) clearly shows the dense vegetation of the poplar farm study area (EVI = 0.66 - 0.99) relative to the surrounding land cover types (EVI = 0.15 - 0.32). The value of every pixel for 2003 and 2004 in each of the three transects is given in Appendix A.
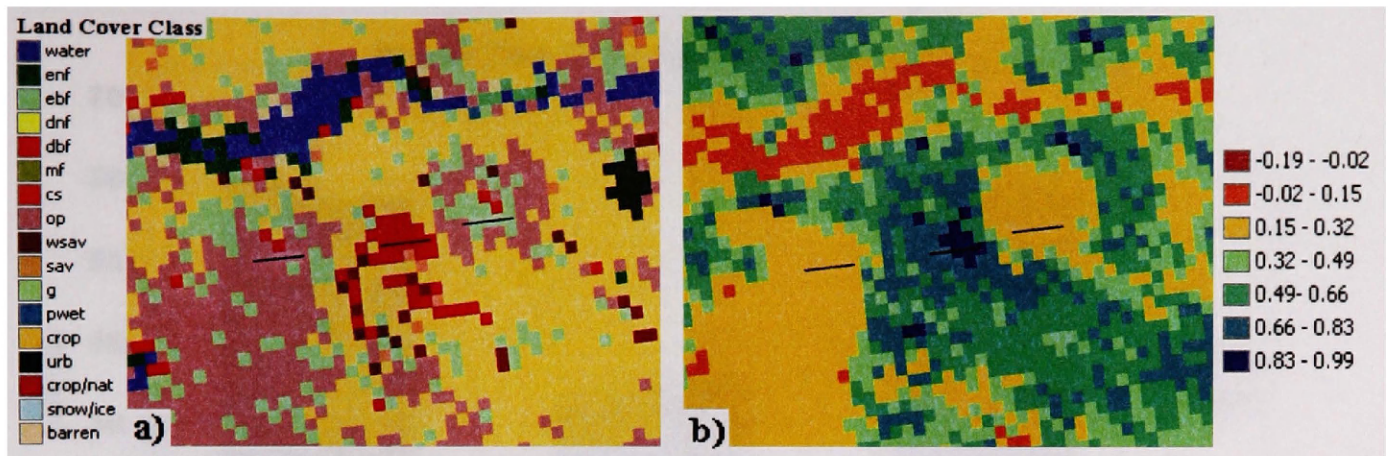
Figure 8. Three transects overlaid on the MODIS Land Cover image (a) and MODIS EVI (b) show the poplar tree farm classified as deciduous broadleaf forest, and with a high EVI compared with the adjacent land cover (open shrubland and grassland).

The poplar tree farm mean-maximum LST for 2003 and 2004 is 33.0°C and 36.0°C and is significantly different from the open shrubland (59.8°C and 57.2°C respectively) and grassland (60.4°C and 59.4°C respectively) land covers with 97% confidence (p = <0.001) (Figure 9). There is no significant difference in mean-maximum LST between the open shrubland and grassland transects.
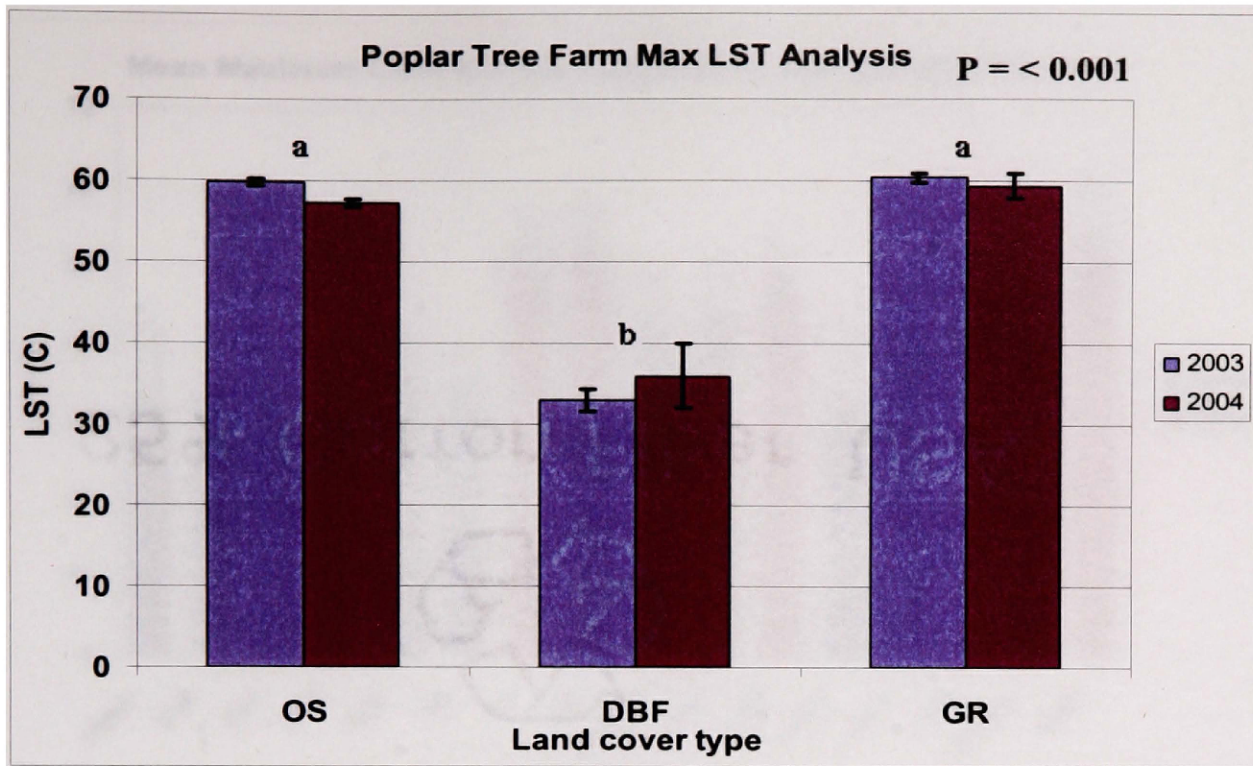
Figure 9. The mean-maximum LST of the poplar tree farm transect (DBF) is significantly different from mean-maximum LST of the open shrubland (OS) and grassland (GR) transects for 2003 and 2004 (p = <0.001).

Biome stratified mean-maximum LST

The mean-maximum LST with one standard deviation for each land cover type during 2003 and 2004 is shown in Figure 10. Land covers highlighted in red indicate that the mean-maximum LST with one standard deviation is at or above 50°C. Barren land cover has a mean-maximum LST of 54.3°C and 52.3°C in 2003 and 2004 respectively, the highest of any land cover type. Open shrubland and closed shrubland covers have a mean-maximum LST of 52.6°C and 50.9°C respectively in 2003. With one standard deviation, savanna, grass, and urban land covers reach the 50°C LST threshold in both years. Forests and permanent wetland cover classes have mean-maximum LSTs below 40°C and are well below 50°C with one standard deviation.

25
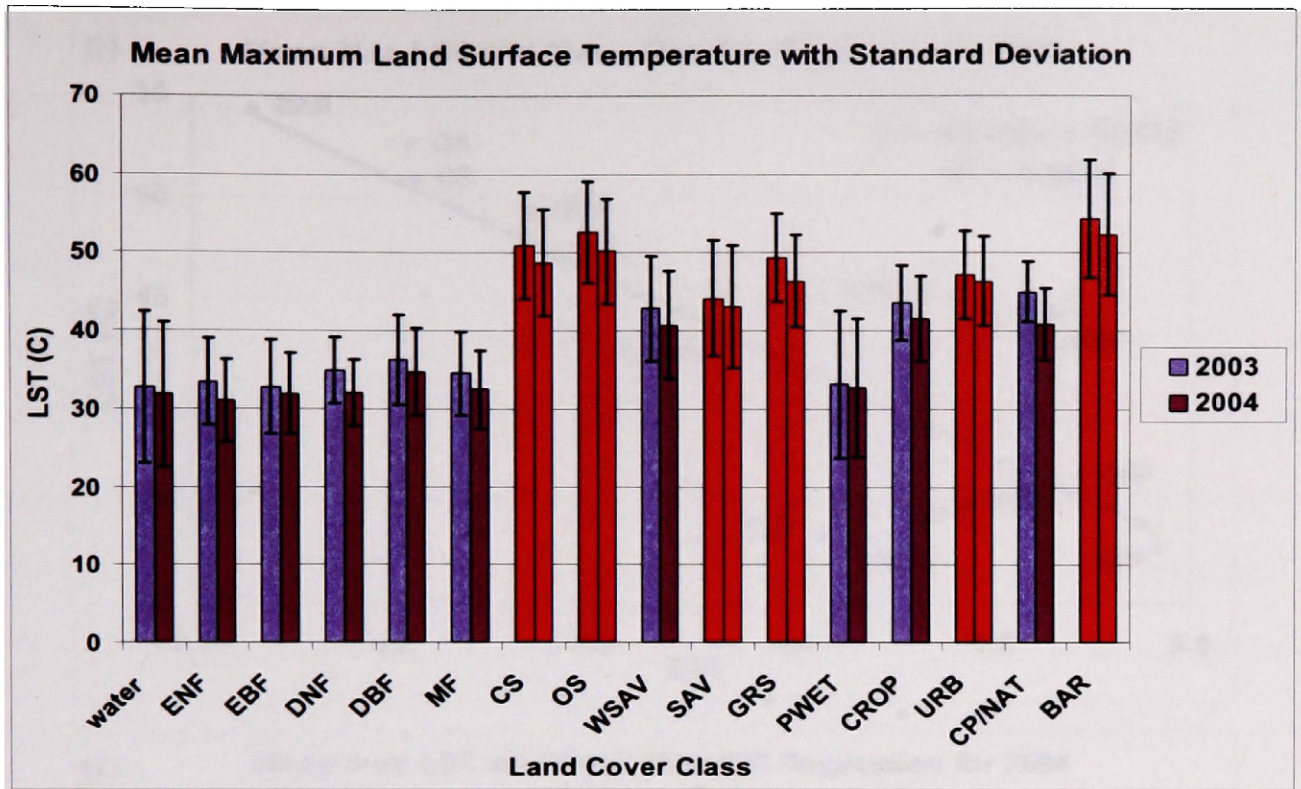
Figure 10. Mean-maximum LST of land cover types in the western U.S. Bars in red represent land cover types with LST and one standard deviation that reach 50°C.

Mean-maximum LST and mean-maximum EVI relationship

The mean-maximum LST and EVI values for each land cover class are given in Appendix B. The land cover class stratified mean-maximum EVI and mean-maximum LST over the entire western United States are strongly negatively correlated ($r = -0.83 \pm .33$) with 95% confidence ($p = < 0.001$) (Table 1). Figure 11 shows the regression between the mean-maximum LST and the mean-maximum EVI with snow and water land cover classes removed for 2003 (a; $R^2 = 0.69$) and 2004 (b; $R^2 = 0.69$).

a) **Mean Max LST and Mean Max EVI Regression for 2003**

LST (C)

$y = -45.362x + 59.975$
$R^2 = 0.6854$

BAR
OS
CS
GRS
URB
CP/NAT
SAV
CROP
WSAV
DBF
MF DNF
ENF
PWET
EBF

55
50
45
40
35
30

0.1   0.2   0.3   0.4   0.5   0.6
EVI

b) **Mean max LST and Mean Max EVI Regression for 2004**

LST (C)

$y = -45.821x + 57.436$
$R^2 = 0.6862$

BAR
OS
CS
URB
GRS
SAV
CROP
WSAV   CP/NAT
DBF
MF
PWET   DNF   EBF
ENF

55
50
45
40
35
30

0.1   0.2   0.3   0.4   0.5   0.6
EVI
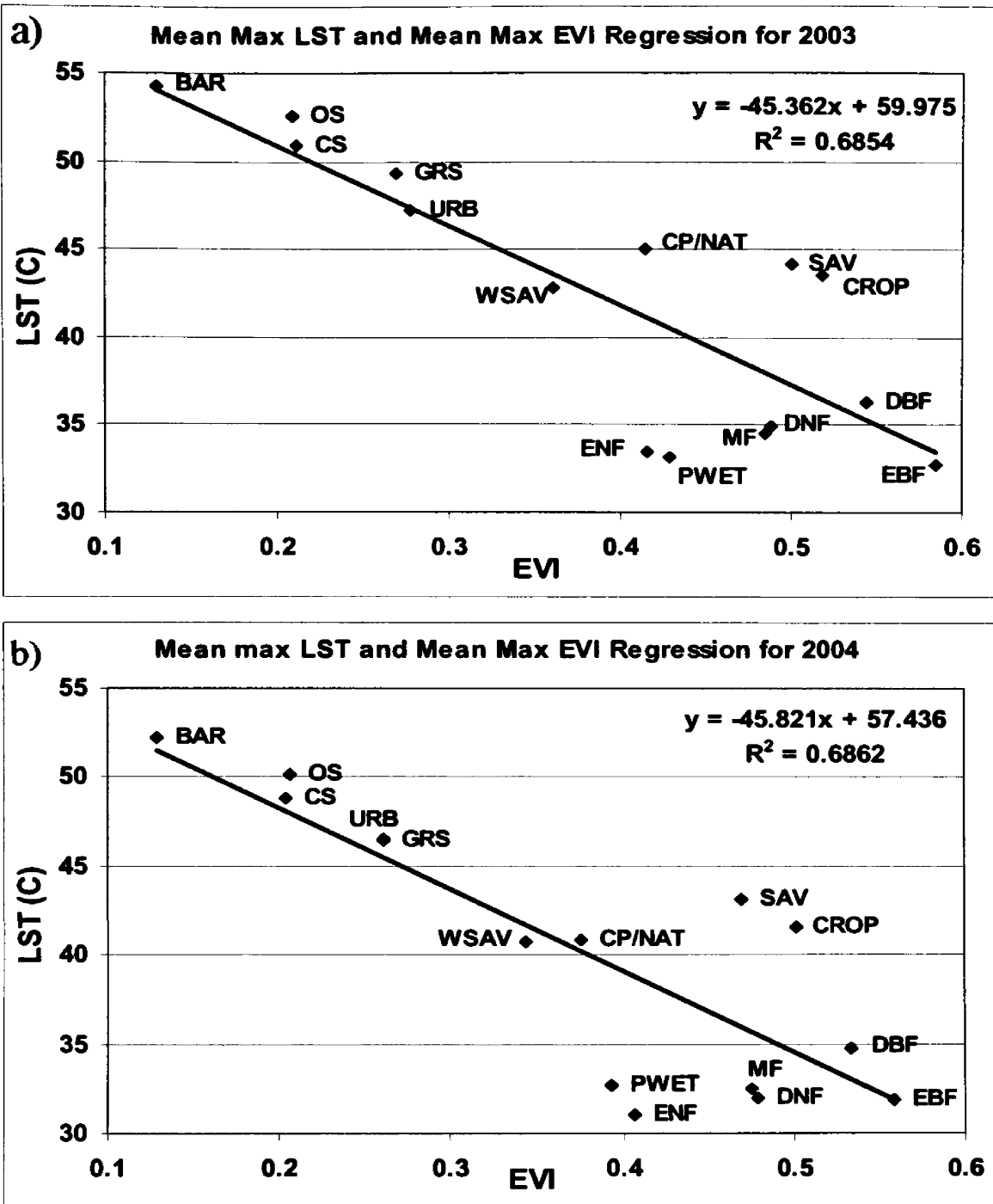
Figure 11. Relationship between mean-max LST and mean-max EVI for all biomes excluding water and snow/ice for the entire study area for 2003 (a) and 2004 (b).

There is a strong negative relationship between the mean-maximum LST and mean-maximum EVI whereby land cover types with low mean-maximum EVI have high mean-maximum LST near or above the 50°C threshold (barren, shrublands and grasslands). On

the opposite end of the energy balance spectrum are land cover types that have high

mean-maximum EVI and low mean-maximum LST (forests and permanent wetlands).

Disturbance Index analysis

The disturbance index results for the western United States study area are shown

in Figure 12. The mean of the entire study area (0.9919) has been rounded to 1.0. The

scale extends from 0.2 to 4.0, and values that are within one standard deviation (0.32) of

the mean are mapped as no color. Values greater than 1.0 mapped in orange and red

indicate that the disturbance index results are 1.0 standard deviation or greater above the

mean. Values less than 1.0 mapped in light blue and dark blue indicate that the

disturbance index results are 1.0 standard deviation or greater below the mean value.
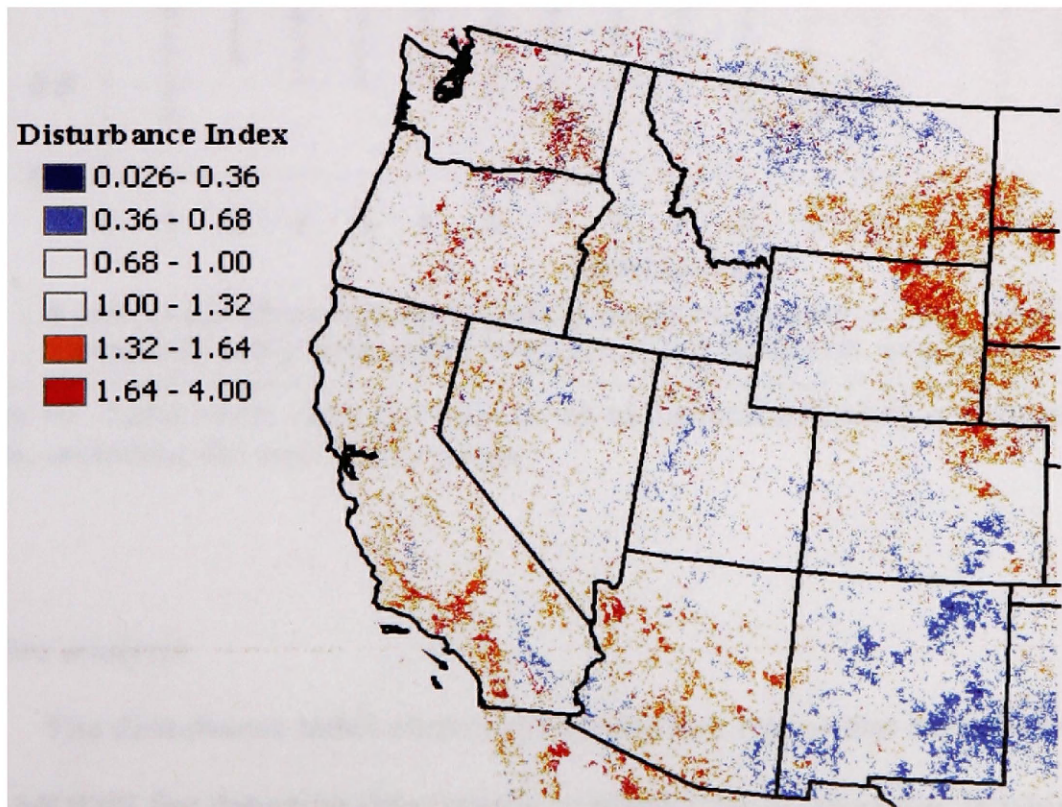
Figure 12. Disturbance index using 1.0 standard deviation (0.32) from the mean (1.0) as
the threshold to indicate disturbance for the western United States.

The scatter-plot illustrates the land cover class stratified mean and standard deviation disturbance index values (Figure 13) and includes the west U.S. average (16). Mean values range between 0.94 and 1.06 for all land cover classes with the exception of permanent wetlands mean value of 1.17. Land cover classes with denser vegetation, such as forests, have lower standard deviations.

Land Cover Stratified Mean Disturbance Index Value

◆ enf (1) ebf (2) dnf (3) dbf (4) mf (5) cs (6) os (7) wsav (8) sav (9) g (10) pwet (11) crop (12) urb (13) crop/nat (14) barren (15) West U.S. avg. (16)
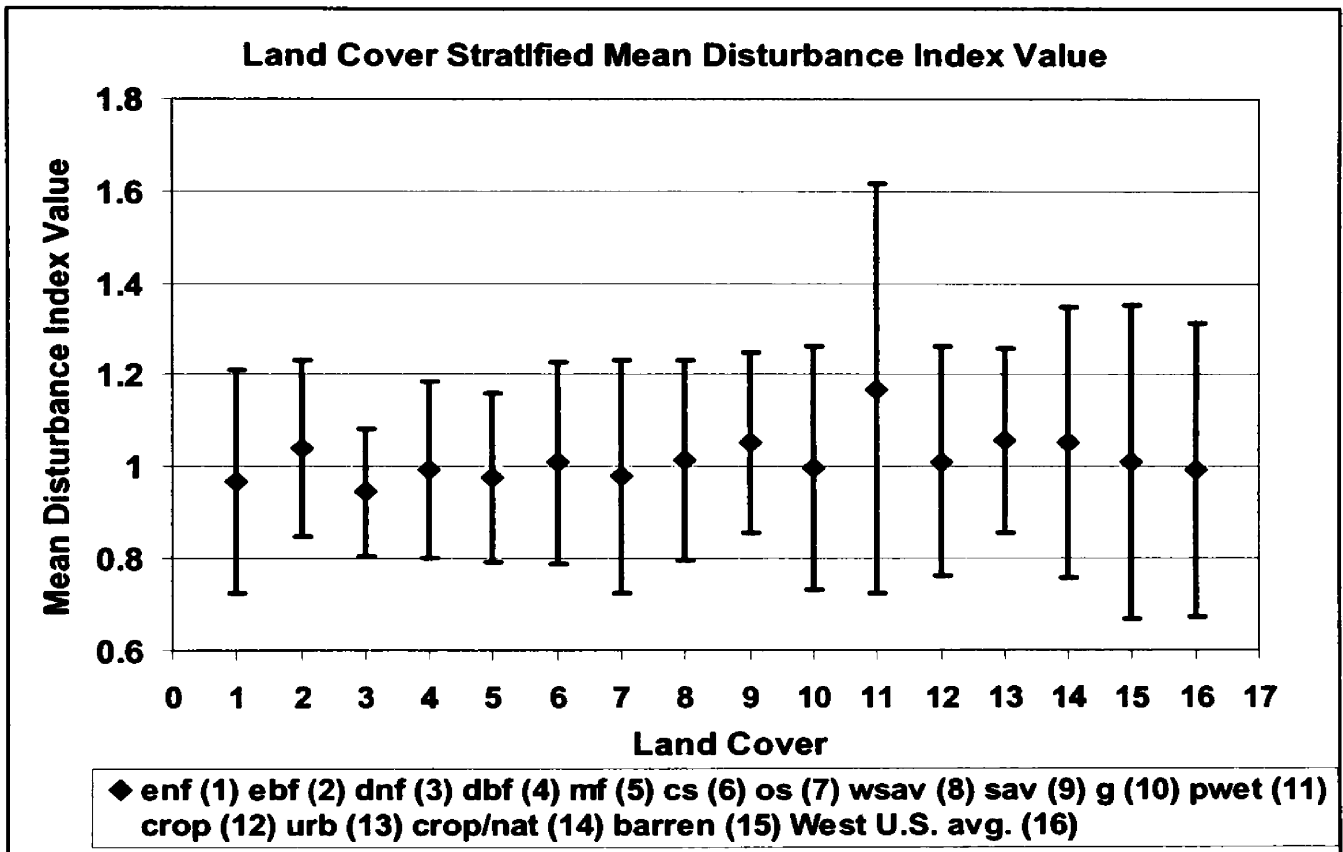
Figure 13. Land cover class stratified mean and standard deviation disturbance index values, including the west U.S. average.

Fire analysis

The disturbance index clearly shows positive values that correspond with the 2003 MODIS fire detection data (shown as black dots) in Montana, Washington, and Oregon (Figure 14).
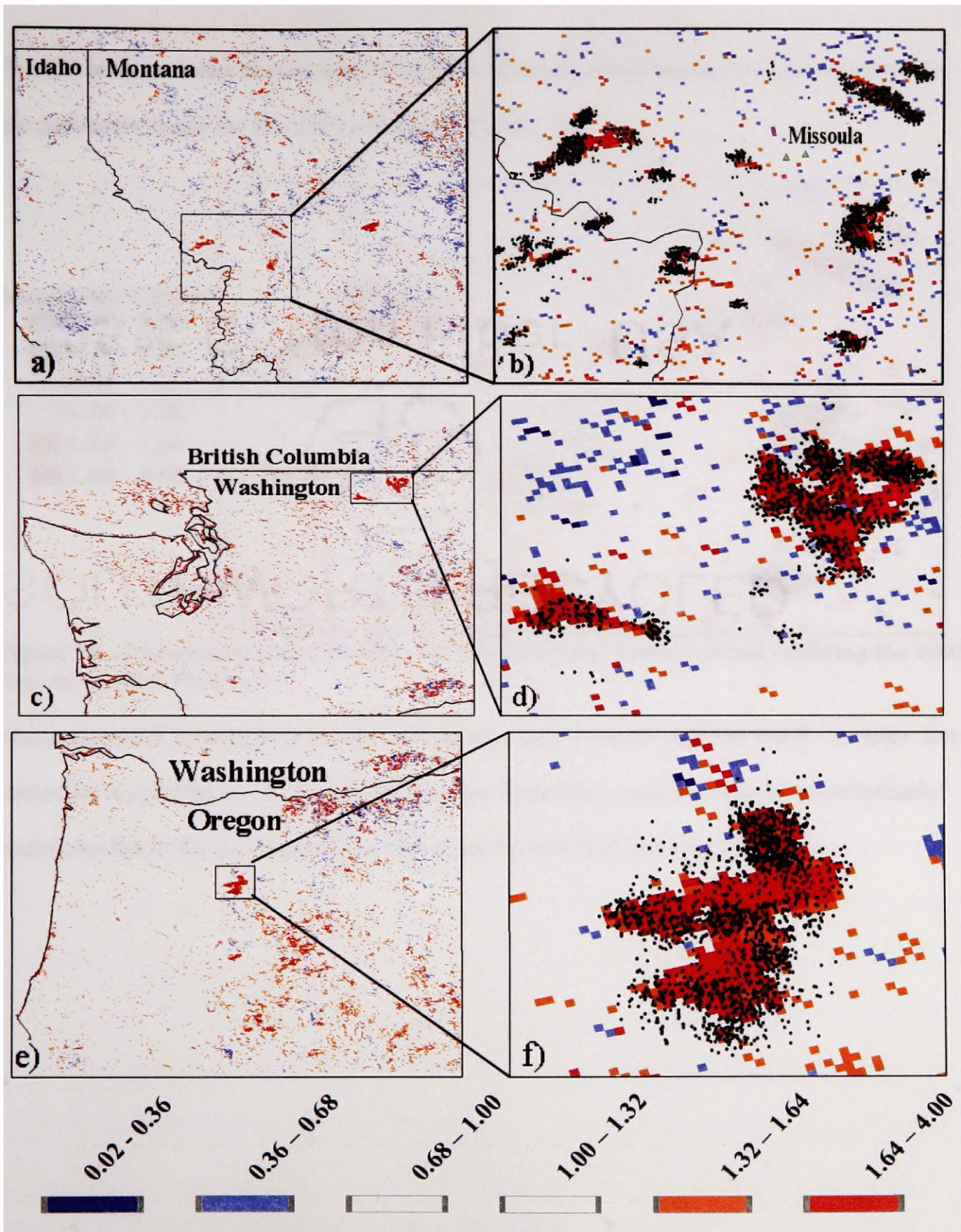
Figure 14. Comparison of disturbance index results with 2003 MODIS fire detection data (black dots) in Montana (a, b), Washington (c, d) and Oregon (e, f).

The disturbance index results near Missoula, Montana show strong similarities with the

fire perimeter maps for the 2003 wildfires (Figure 15).
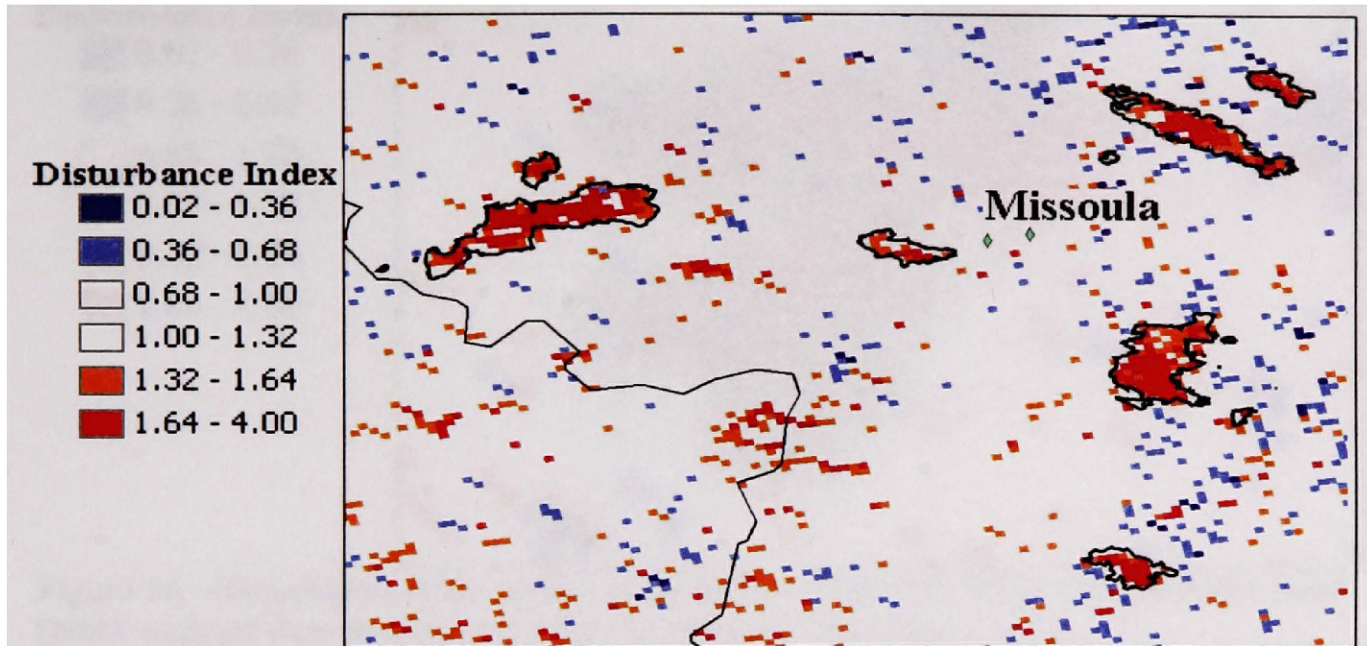
Figure 15. Disturbance index results with fire perimeter maps overlaid outlining the 2003 fires in western Montana.

The same result is seen between the disturbance index results and the B&B Complex fire

perimeter map (Figure 16). Furthermore, the disturbance index results more accurately

match the B&B fire perimeter map than does the MODIS fire detection data.

Disturbance Index

- 0.02 - 0.36
- 0.36 - 0.68
- 0.68 - 1.00
- 1.00 - 1.32
- 1.32 - 1.64
- 1.64 - 4.00
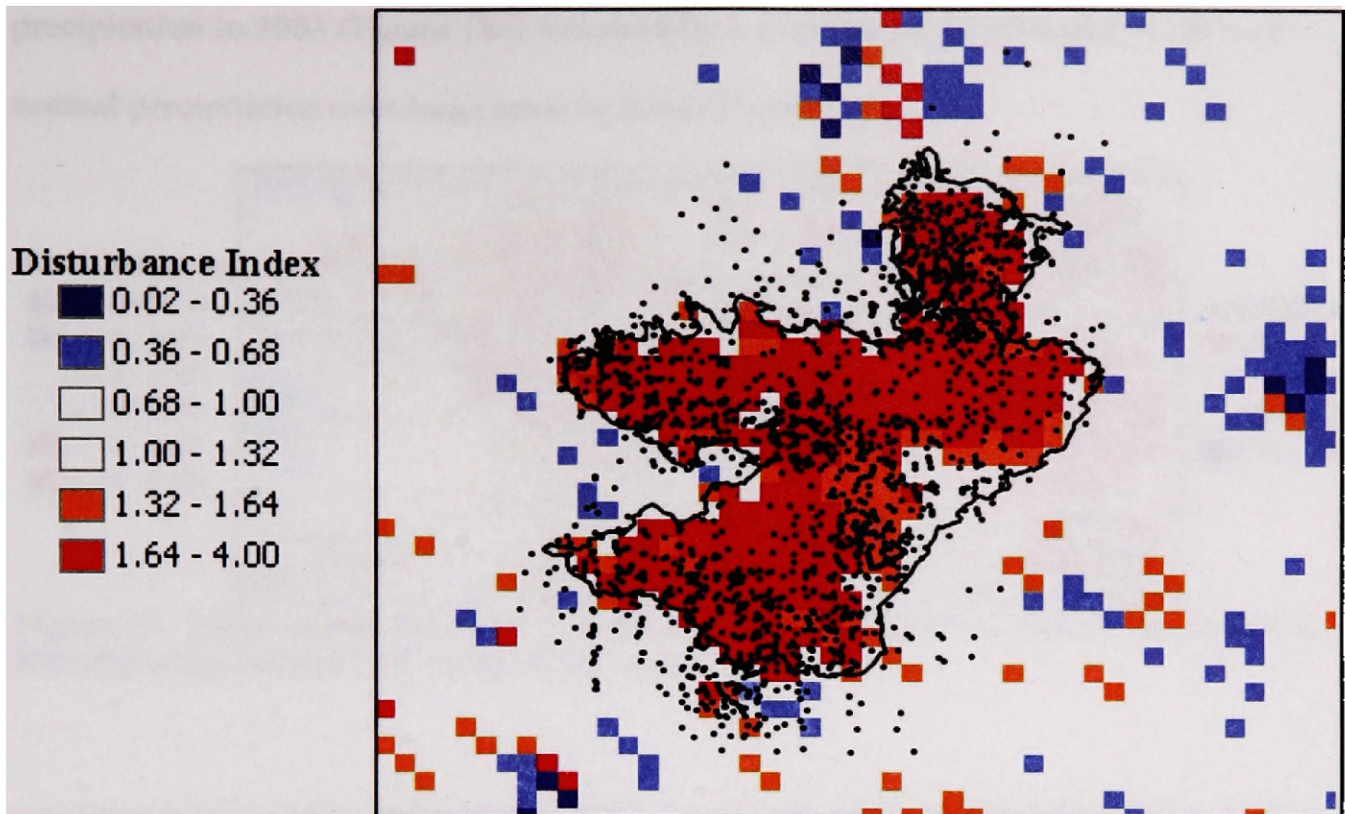
Figure 16. Disturbance index results more closely match the B&B fire perimeter map (black outline) than does the MODIS fire detection data (black dots).

Interior Northwest region

A large disturbed area seen in orange and red (Figure 17a) extends throughout Southeast Montana, Northeast Wyoming, Southwest North Dakota and West South Dakota. This area has disturbance index values greater than 1.0 standard deviation above the mean indicating that the 2004 LST/EVI ratio was greater than the 2003 ratio. A *max-EVI ratio map* (2004 max EVI/2003 max EVI) was created that shows whether EVI went up or down over the two-year study period. The *max-EVI ratio map* shows that the interior northwest (NW) region of the study area had a decrease in EVI from 2003 to 2004 and that these patterns are similar to the disturbance index results (Figure 17b). This agrees with precipitation anomaly maps that show this region receiving average

precipitation in 2003 (Figure 18a) followed by a decrease to 51-70% and 71-90% of

normal precipitation over large areas in 2004 (Figure 18b).
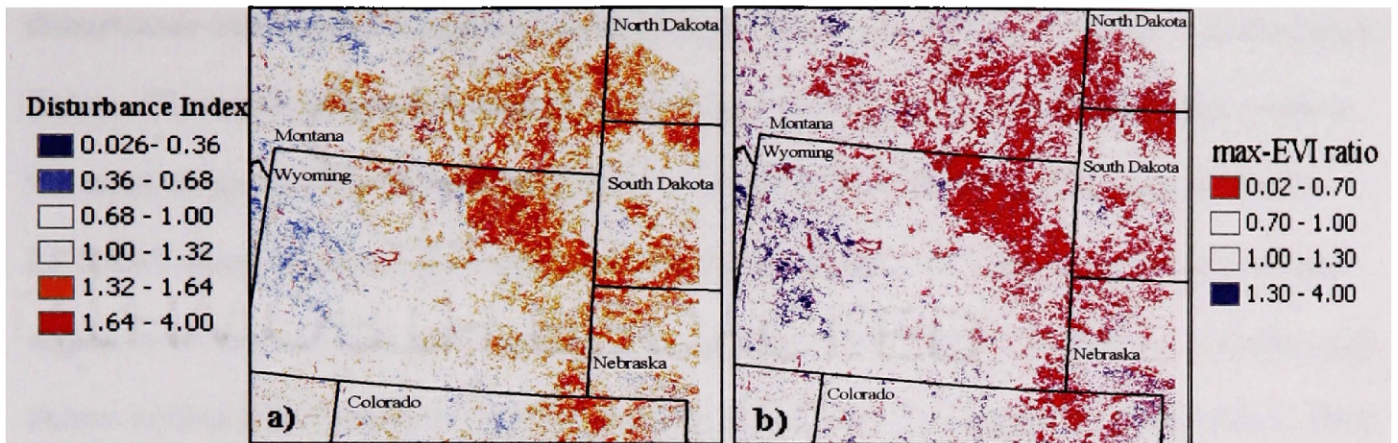
Figure 17. Index results (a) show disturbance patterns that are similar to the decline in EVI (b) in the interior NW of the study area.
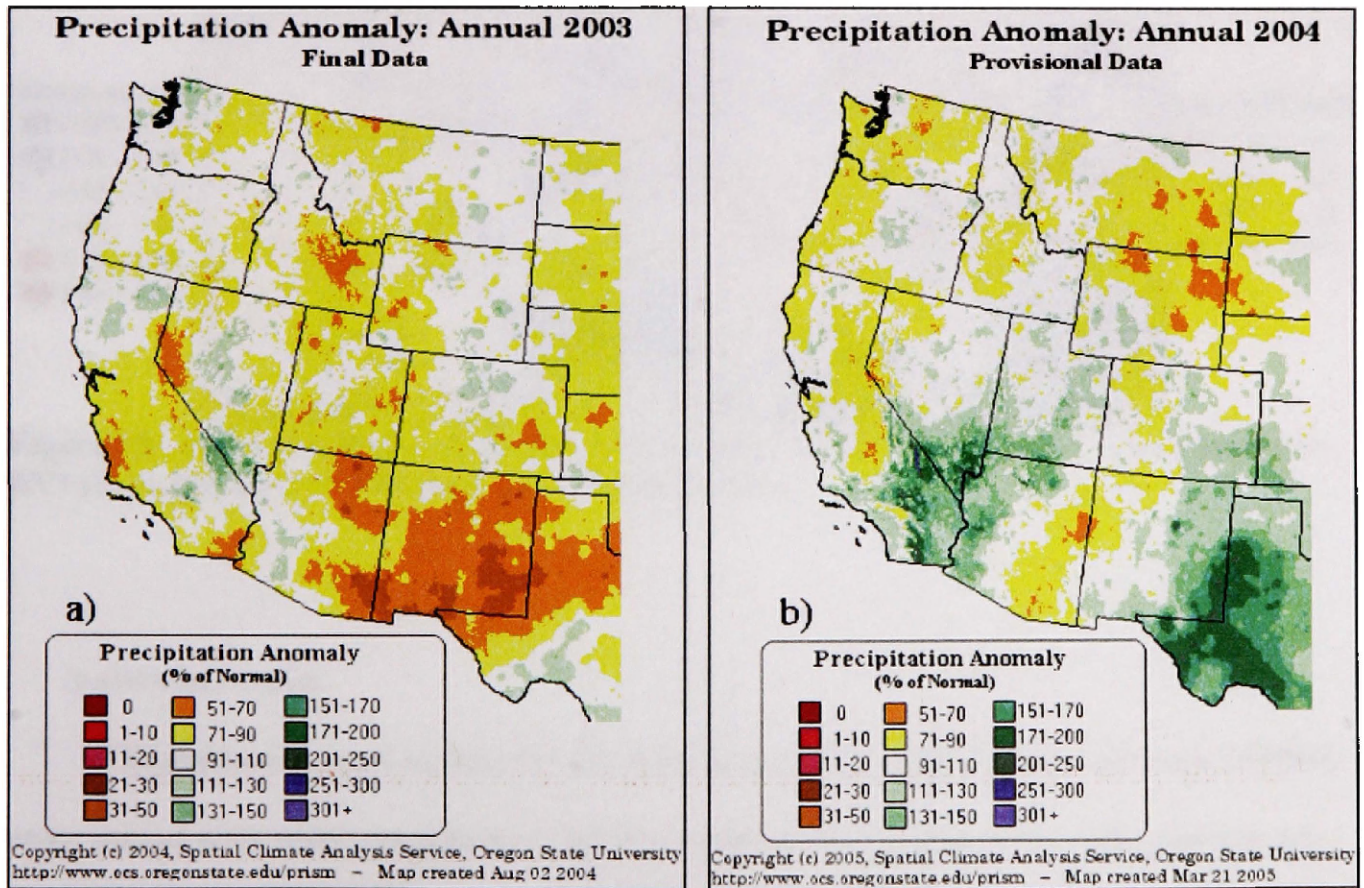
Figure 18. Precipitation anomaly maps for 2003 (a) and 2004 (b) for the western U.S.

Interior Southwest region

Results from the interior southwest (SW) part of the study area show a large disturbance extending throughout much of New Mexico, Southern Colorado, and western Texas. The areas mapped in blue have values greater than 1.0 standard deviation below the mean (Figure 19a), indicating that the 2004 LST/EVI ratio was less than the 2003 LST/EVI ratio. The *max-EVI ratio map* shows an increase in vegetation density in this region over the two-year study period (Figure 19b). The 2003 precipitation anomaly map shows widespread deficits in precipitation in the interior SW region, 31-50% and 51-70% of normal (Figure 18a). In 2004, the same area received as much as 171-200% of normal precipitation (Figure 18b).
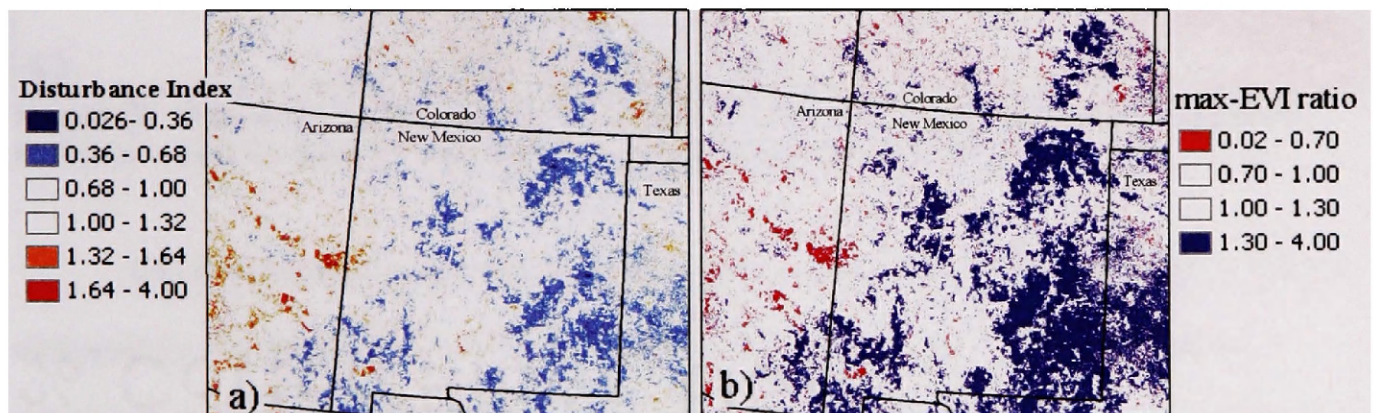
Figure 19. Index results (a) show disturbance patterns that are similar to the increase in EVI (b) in the interior SW portion of the study area.

Southwest region

Disturbance index results for the southwest (SW) region consist of large wildfire scars mixed with index responses of various trajectories (Figure 20a). The patterns are very similar to the *max-EVI ratio* map (Figure 21) with the exception of the 2003 wildfire scars (Figure 20c,d). A *max-LST ratio map* (2004 max LST/2003 max LST) was created

that shows whether LST went up or down over the two-year study period. The *max-LST ratio map* for the SW part of the study area draws out the 2003 wildfire patterns remarkably well (Figure 20b). These wildfires were in a mixture of open shrubland, closed shrubland, woody savanna, savanna, grasslands and evergreen needleleaf forest. While wildfire patterns from other parts of the study area do emerge in the *max-LST ratio map*, none have as clear a signal as in this landscape.
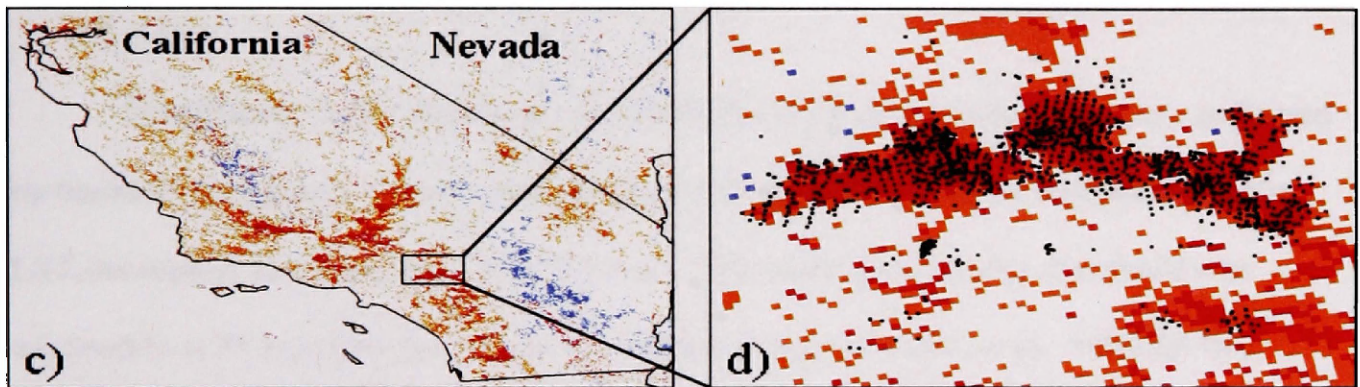
Figure 20. Southern California's 2003 wildfires show up clearly with the disturbance index (a, c and d) and LST increased in the fire areas in 2004 (b).

The disturbance index results in the southern Sacramento Valley (Figure 21a) are mirrored by the decline in EVI from 2003 to 2004 (Figure 21b). The precipitation anomaly maps shows that precipitation deficit in the central Sacramento Valley during 2003 (Figure 18a), moved southward in 2004 (Figure 18b). In south-central California, below normal precipitation in 2003 was followed by 131% to 170% of normal precipitation in 2004. The *max-EVI ratio map* shows that vegetation density increased in the same area in 2004 (Figure 21b). The patterns of increasing EVI correspond with the disturbance index results (Figure 21a).
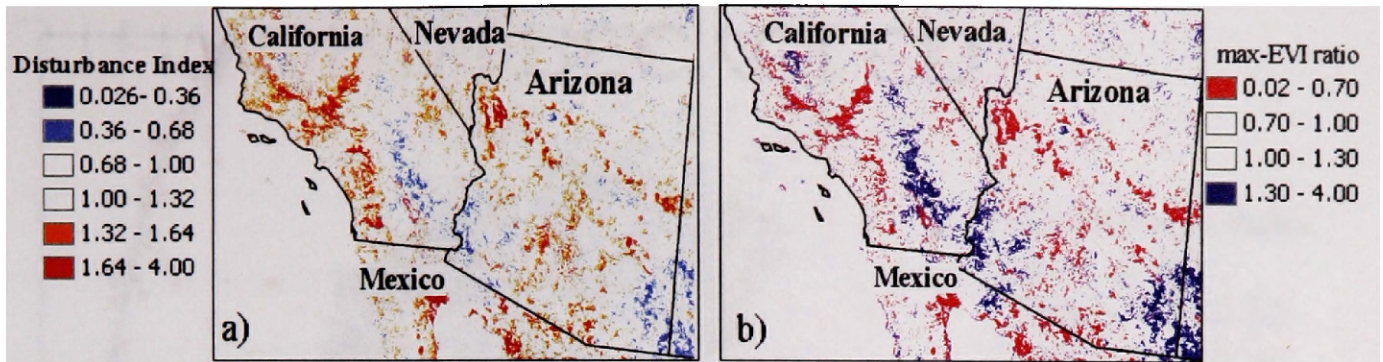
Figure 21. Disturbance index results (a) match patterns of EVI interannual change (b) with the exception of the wildfire scars, which resemble interannual LST variability.

Recovery

Disturbance index results for the 2002 Biscuit Fire area show recovery indicated by the blue disturbance index results (Figure 22). The EVI in 2004 increased and the LST decreased, lowering the LST/EVI ratio. The disturbance index threshold was adjusted to 0.75 standard deviations to evaluate recovery in this area. MODIS fire detection points are shown overlaid on the fire area. Recovery is found coinciding with the 2002 MODIS fire detection data throughout the western U.S.
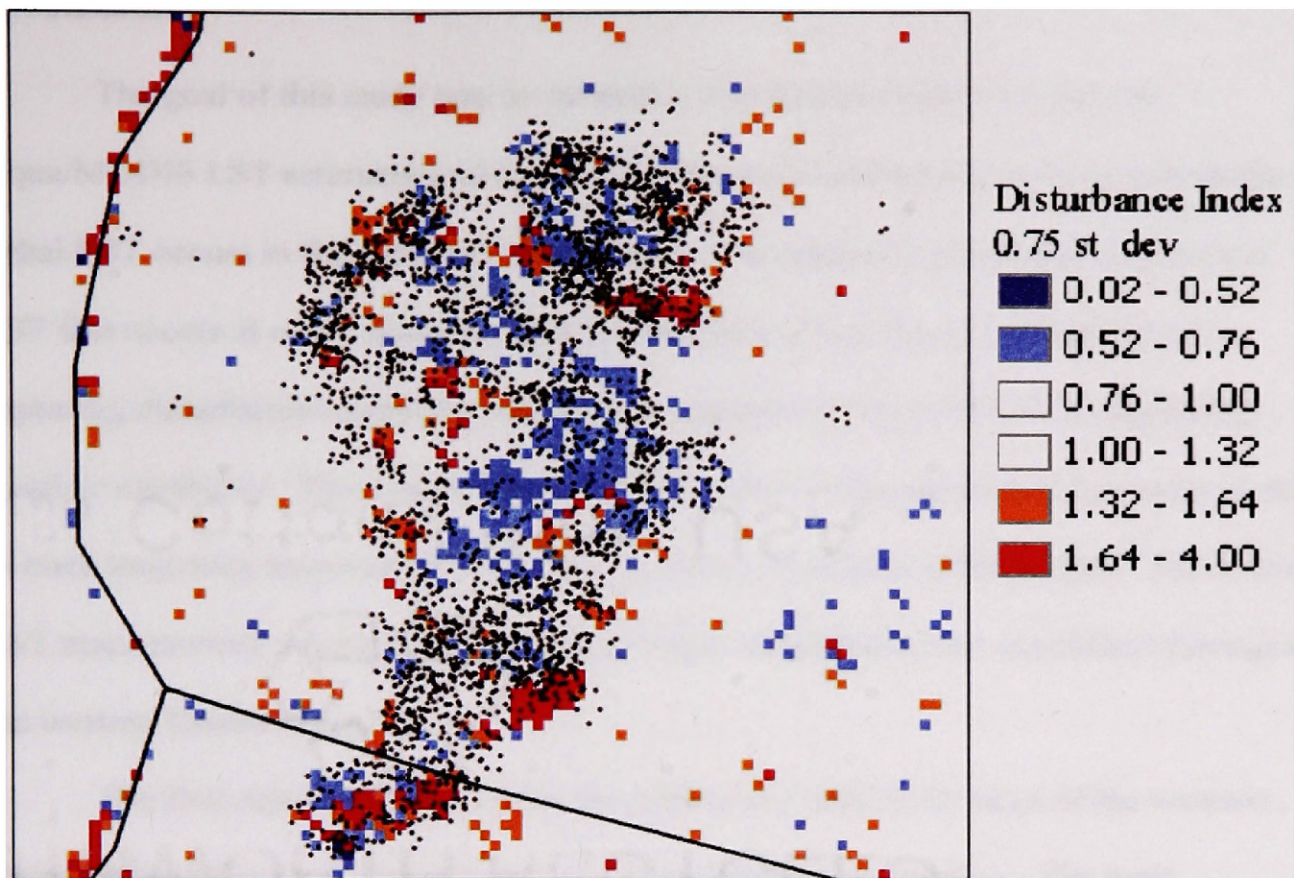
Figure 22. Recovery seen in blue indicates an increase in EVI and decrease in LST from 2003 to 2004 in the 2002 Biscuit Fire Area in Southwest Oregon's Siskiyou Mountains.

Discussion

The goal of this study was to develop a disturbance index that uses the Aqua/MODIS LST estimates and to identify where physiologically defined potentially lethal LST occurs in the western United States. The approach of using the maximum LST that occurs at every pixel during an annual period has shown to be effective in capturing disturbance caused by wildfire and impacts on vegetation from interannual weather variability. This suggests that the disturbance index developed here may be able to track long-term incrementally developing trends associated with drought. The extreme LST maps provide a fresh look into how extreme temperatures are distributed throughout the western United States.

The first objective was to generate potentially lethal LST maps of the western United States (Figure 3) and interpret the major bioclimatic patterns. The main bioclimatic factors controlling lethal LST patterns are elevation, continentality, latitude, and land cover type. The maritime influence moderates temperature along the coast, and in the Pacific Northwest, where average annual rainfall is high and dense forest blankets much of the region, latent heat flux plays an important role in keeping temperature well below the lethal threshold. Forests are very effective at moderating LST and generally stay below 40°C throughout the entire study area (Figure 10). The timing of acquisition for maximum LST (Figure 6) clearly illustrates that cloud cover is not causing temporally biased acquisitions that might confound interpretation of the major bioclimatic patterns of extreme LST.

All land cover types (excluding water and snow/ice) in the interior western United States commonly reach 50°C with the exception of forests, permanent wetlands, and

agricultural areas. However, interannual variability with regards to the spatial

distribution of potentially lethal LST can be high, as it was between 2003 and 2004

(Figure 3). Irrigated agricultural areas allow for transpiration to stay high when it

otherwise would decrease or shut down. This dissipates energy through latent heat flux

and maintains low LST. The Sacramento Valley is a good example, as the agricultural

areas of the valley do not reach the potentially lethal threshold. The border between the

forest and the agricultural lands is woody savanna, and tends to reach 50°C or greater. If

it were not for the land cover conversion of the Sacramento Valley to agricultural lands, it

is likely that the majority of the valley would reach 50°C or greater. This large-scale

manipulation of extreme LST patterns may have implications for survival of pests and

diseases that otherwise could not complete their life cycle due to extreme temperature

exposure.

The second objective of this project was to assess the accuracy and sensitivity of

the disturbance index using independent data sources. The maximum LST sensitivity

analysis suggests that the Aqua/MODIS LST estimates are capable of detecting LST

variation associated with vegetation density gradients at a fine-scale. The vegetation

density gradient is very strong (Figure 8b) in the poplar tree farm LST sensitivity

analysis. The significant difference between the maximum LST of the poplar tree

plantation and the maximum LST of the adjacent open shrubland and grassland cover

types supports the principle that surface temperature decreases with an increase in

vegetation density through latent heat transfer (Figure 9). This is further supported at the

regional-scale by the strong and negative relationship between the mean-maximum LST

and the mean-maximum EVI (R^2 = .69; Figure 11) found throughout the study area. The logic of the disturbance index is based on this relationship.

The energy balance of a given land cover is controlled by the partitioning of incoming solar radiation into latent and sensible heat fluxes. If water is available to transpire, as it is for much of the year in forests, then the maximum LST will not reach 45°C (Figure 10). Disturbance alters vegetation, and therefore, the major mechanism through which latent heat transfer occurs. If vegetation is damaged or destroyed, incoming solar radiation is partitioned more towards sensible heat flux, and LST increases. In the case of the poplar tree farm, irrigation results in a positive disturbance where vegetation increases, and LST decreases. Because biomes have different strategies for recovering from disturbance such as wildfire, (e.g. Chaparral species can resprout from carbohydrate-rich root burls, whereas pine forests regenerate from seed) recovery time of ecosystems, in terms of restoration of the energy balance of a site, varies. The ratio of maximum LST to maximum EVI takes into account both the major mechanism through which latent heat transfer occurs, the vegetation, and the energy partitioning itself, LST. This optimizes the ability of the disturbance index to work over broad scales and various biomes as seen in this project. Potter et al. (2003) in a global evaluation of disturbance events using an 18-year Advanced Very High Resolution Radiometer dataset observed that vegetation classes with the highest frequency of major disturbance are savannas, shrublands, and coniferous (boreal) forests. The clarity with which the maximum LST interannual variability clearly distinguishes the 2003 California wildfires (Figure 20a) in a savanna and shrubland vegetation type suggest that the LST/EVI

disturbance index is capable of detecting disturbance in the Earth's most frequently disturbed land cover types.

The two years encompassed by this study happen to have been a very dry year (2003) and a very wet year (2004). The index results capture disturbance patterns caused by interannual weather variability and this particular response of the disturbance index appears to be primarily driven by the interannual variability in the EVI. Grasslands were particularly effected by interannual weather variability most likely due to their shallow root systems. Open shrublands and cropland/natural vegetation mosaic also tend to be more susceptible to interannual weather variability.

Disturbance index results show recovery associated with the 2002 fire areas identified by the MODIS fire detection. The recovery signal is weaker compared to disturbance as recovery is a longer and more incremental process than most disturbance processes. The disturbance index threshold was adjusted from 1.0 standard deviation from the mean, to 0.75, resulting in a more clear recovery pattern associated with the 2002 MODIS fire detection data (Figure 22). However, more noise accompanied this threshold value change throughout the study area. It is important to point out that the disturbance index threshold for disturbance recovery may be different than the threshold for disturbance detection. The ability to assess the disturbance index recovery results is limited by the two years of data.

Conclusions

Accelerating climate change makes the relationship between stress physiology, and LST as related to current and future distributions of organisms an area of critical importance. The potentially lethal LST maps provide a new tool for researching many of these critical questions. Clearly, if the trend toward drier summers and higher LST continues, extreme LST will cover a greater areal extent and begin to have greater effects on species that have not adapted to such temperatures. Forests on ecotones with drier biomes such as grasslands and open shrublands could become more strongly affected by extreme LST. Post-disturbance recovery of forest ecosystems could become more problematic if extreme LST causes mortality to seedlings due to soil insolation. Field studies exploring soil insolation caused mortality to tree seedlings in post-disturbance forest ecosystems would help to resolve this issue.

This study suggests that the disturbance index algorithm is flexible and effective at monitoring various types of land surface disturbance throughout the diverse bioclimatic regions of the western U.S. The energy balance approach to disturbance monitoring likely holds the key to an improved disturbance metric for continental change detection. This study has affirmed that disturbance does generate a large enough LST/EVI signal for the disturbance index presented here to detect and that the signal is bigger than the natural variability. Disturbance due to wildfire and precipitation variability both generate large enough signals to detect in different regions across the study area. Natural variability appears to be generally less than 1.0 standard deviation from the mean disturbance index value. Given the need for a global disturbance

monitoring tool, further investigation of the disturbance algorithm over longer time periods and at the global scale is warranted.

References

Baker, F.S., 1929. Effect of excessively high temperatures on coniferous reproduction. Journal of Forestry, 27: 949-975.

Barnes, V.B., Zak, D.R., Denton, S.R. and Spurr, S.H., 1998. Forest Ecology. John Wiley and Sons, Somerset, NJ.

Canadell, J.G. et al., 2000. Carbon metabolism of the terrestrial biosphere: a multi-technique approach for improving understanding. Ecosystems, 3: 115-130.

Crag, R., Sugita, M. and Brutsaert, W., 1995. Satellite-derived surface temperatures with boundary layer temperatures and geostrophic winds to estimate surface energy fluxes. Journal of Geophysical Research, 100(D12): 25447-25451.

Davis, M.B. and Zabinski, C., 1992. Change in geographical range resulting from greenhouse warming: Effects on biodiversity in forests. In: R.L. Peter and T.E. Lovejoy (Editors), Global Warming and Biological Diversity. Yale University Press, New Haven, CT.

Diak, G.R. and Whipple, M.S., 1993. Improvements to models and methods for evaluating the land-surface energy balance and effective roughness using radiosonde reports and satellite-measured skin temperature data. Agricultural and Forest Meteorology, 63(3-4): 189-218.

Dozier, J. and Warren, S.G., 1982. Effect of viewing angle on the infrared brightness temperature of snow. Water Resources Research, 18(5): 1424-1434.

Dyer, J.M., 1995. Assessment of climatic warming using a model of forest species migration. Ecological Modeling, 79: 199-219.

Flenley, J.R., 1998. Tropical forests under the climates of the last 30,000 years. Climatic Change, 39: 177-197.

Gates, D.M., 1980. Biophysical Ecology. Springer-Verlag, New York, 611 pp.

Goetz, S.J., 1997. Multi-sensor analysis of NDVI, surface temperature and biophysical variables at a mixed grassland site. International Journal of Remote Sensing, 18: 71-94.

Goward, S.N., Cruickshank, G.D. and Hope, A.S., 1985. Observed relation between thermal emission and reflected spectral radiance of a complex vegetated landscape. Remote Sensing of Environment, 18: 137-146.

Houghton, J.T. et al., 1996. Climate Change 1995 - The Science of Climate Change: Second Assessment Report of the Intergovernmental Panel on Climate Change. Cambridge University Press, Cambridge.

Iverson, L.R., Prasad, A.M., Hale, B.J. and Sutherland, E.K., 1999. Atlas of Current and Potential Future Distributions of Common Trees of the Eastern United States. General Technical Report NE-265, U.S. Department of Agriculture, Forest Service, Radnor, PA.

Kattenburg, A. et al., 1996. Climate models-projections of future climate. In: J.T. Houghton et al. (Editors), Climate Change 1995: The Science of Climate Change. Cambridge University Press, Cambridge, pp. 285-358.

Labed, J. and Stoll, M.P., 1991. Angular variation of land surface spectral emissivity in the thermal infrared: laboratory investigations on bare soils. International Journal of Remote Sensing, 12(11): 2299-2310.

Lange, O.L. and Lange, R., 1963. Untersuchungen uber Blattemperaturen, Transpiration und Hitzeresistenz an Pflanzen mediterraner Standorte. Flora (Jena), 153: 387-425.

Larcher, W., 2003. Physiological Plant Ecology. Springer-Verlag, New York.

Levitt, J., 1941. Frost Killing and Hardiness of Plants. Burgess, Minneapolis, MN.

Levitt, J., 1980. Responses of Plants to Environmental Stress, 1. Academic Press, New York.

Li, Z.-L. and Becker, F., 1993. Feasibility of land surface temperature and emissivity determination from AVHRR data. Remote Sensing of Environment, 43: 67-85.

Lorenz, R.W., 1939. High Temperature Tolerance of Forest Trees. Technical Bulletin 141, University of Minnesota Agricultural Experiment Station, Minneapolis, MN.

Lundegardh, H., 1949. Klima und Boden. Fischer, Jena.

Mannstein, H., 1987. Surface energy budget, surface temperature and thermal intertia. In: R.A. Vaughan and D. Reidel (Editors), Remote Sensing Applications in Meteorology and Climatology. NATO ASI Series C: Mathematical and Physical Sciences. Reidel, Dordrecht, Netherlands, pp. 391-410.

McCarthy, J.J., Canziani, O.F., Leary, N.H., Dokken, D.J. and White, K.S., 2001. Climate Change 2001: Impacts, Adaptation and Vulnerability. Cambridge University Press, Cambridge.

45

McFarland, M.J., Miller, R.L. and Neale, C.M.U., 1990. Land surface temperature derived from the SSM/I passive microwave brightness temperatures. IEEE Trans. Geosci. Remote Sensing, 28(5): 839-845.

MODIS Science Team: LST-Group, 2003. MODIS Land Surface Temperature Products Users' Guide. < http://www.icess.ucsb.edu/modis/LstUsrGuide/usrguide.html>.

MODIS Science Team: TBRS Lab, 2003. MODIS Vegetation Product Users' Guide. < http://tbrs.arizona.edu/project/MODIS/UserGuide_doc.php>.

Munch, E., 1913. Hitzeschaden an Waldpflanzen. Naturwiss. Z. Forst.- Landwirtsch, 11: 557-562.

Nemani, R.R., Pierce, L.L. and Running, S.W., 1993. Developing satellite-derived estimates of surface moisture status. Journal of Applied Meteorology, 32: 548-557.

Nemani, R.R. and Running, S.W., 1988. Estimation of Regional Surface Resistance to Evapotranspiration from NDVI and Thermal-IR AVHRR Data. Journal of Applied Meteorology, 28: 276-284.

Nemani, R.R. and Running, S.W., 1997. Land Cover Characterization Using Multitemporal Red, Near-IR, and Thermal-IR Data from NOAA/AVHRR. Ecological Applications, 7(1): 79-90.

Picket, S.T.A. and White, P.S., 1985. The Ecology of Natural Disturbance as Patch Dynamics. Academic Press, New York.

Potter, C. et al., 2003. Major Disturbance Events in Terrestrial Ecosystems Detected using Global Satellite Data Sets. Global Change Biology, 9(7): 1005-1021.

Rees, W.G. and James, S.P., 1992. Angular variation of the infrared emissivity of ice and water surfaces. International Journal of Remote Sensing, 13: 2873-2886.

Running, S.W. et al., 1994. Terrestrial remote sensing science and algorithms planned for EOS/MODIS. International Journal of Remote Sensing, 15(17): 3587-3620.

Saxe, H., Cannell, M.G.R., Johnsen, O., Ryan, M.G. and Vourlitis, G., 2001. Tree and forest functioning in response to global warming. New Phytologist, 149: 369-400.

Sellers, P.J., Hall, F.G., Asrar, G., Strebel, D.E. and Murphy, R.E., 1988. The first ISLSCP Field Experiment (FIFE). Bulletin of the American Meteorological Society, 69(1): 22-27.

Shriner, D.S. and Street, R.B., 1998. North America. In: R.T. Watson, M.C. Zinyowera, R.H. Moss and D.J. Dokken (Editors), The Regional Impacts of Climate Change. An Assessment of Vulnerability. Cambridge University Press, Cambridge, pp. 253-330.

Shukla, J. and Mintz, Y., 1982. Influence of land-surface evapotranspiration on the earth's climate. Science, 215: 1498-1501.

Tilman, D., 1985. The resource-ratio hypothesis of plant succession. American Naturalist, 125: 827-852.

Turner, N.C. and Kramer, P.J., 1980. Adaptations of Plants to Water and High Temperature Stress. John Wiley and Sons, New York.

Wan, Z., 1999. MODIS Land-Surface Temperature Algorithm Theoretical Basis Document (LST ATBD) Version 3.3, 73 pp.

Wan, Z. and Dozier, J., 1989. Land-surface temperature measurement from space: physical principles and inverse modeling. IEEE Trans. Geosci. Remote Sensing, 27(3): 268-278.

Wan, Z. and Dozier, J., 1996. A generalized split-window algorithm for retrieving land-surface temperature from space. IEEE Trans. Geosci. Remote Sensing, 34: 892-905.

Wan, Z., Zhang, Y., Zhang, Q. and Li, Z.-L., 2004. Quality assessment and validation of the MODIS global land surface temperature. International Journal of Remote Sensing, 25(1): 261-274.

Williams, D.W. and Liebhold, A.M., 1997. Latitudinal shifts in spruce budworm (Lepidoptera: Tortricidae) outbreaks and spruce-fir forest distributions with climate change. Acta Phytopathologica et Entomologica Hungarica, 32: 205-215.

List of Tables

Table 1. Correlation results for land cover class stratified mean-maximum LST and mean-maximum EVI.

Correlation Results						
	n	r	p-value	Sr	t(alpha/2,df)	CL
alpha = 0.05						
LST/EVI	15	0.828	<0.001	0.156	2.145	0.334

Appendix A

Maximum LST sensitivity analysis pixel data and averages for three transects during 2003 and 2004

	Transects		
	Open Shrubland	Deciduous Broadleaf Forest	Grassland
2003 LST (°C)	59	34	60
	60	32	61
	60	32	60
	60	32	61
	60	35	60
2003 Avg. (°C)	59.8	33.0	60.4
2004 LST (°C)	57	34	57
	57	32	60
	57	34	60
	57	42	61
	48	38	59
2004 Avg. (°C)	57.2	36.0	59.4

Appendix B

Biome stratified mean-maximum EVI and mean-maximum LST with 1.0 standard deviation for 2003 and 2004

Land Cover	2003				2004			
	EVI max	St dev	LST max	St dev	EVI max	St dev	LST max	St dev
ENF	0.415	0.116	33.436	5.509	0.406	0.107	31.056	5.27
EBF	0.585	0.138	32.706	6.048	0.559	0.132	31.908	5.148
DNF	0.488	0.081	34.899	4.325	0.479	0.084	31.983	4.285
DBF	0.544	0.111	36.264	5.728	0.534	0.11	34.735	5.678
MF	0.484	0.109	34.545	5.354	0.475	0.105	32.487	5.022
CS	0.211	0.091	50.922	6.85	0.203	0.084	48.753	6.793
OS	0.208	0.101	52.629	6.408	0.206	0.096	50.187	6.715
WSAV	0.361	0.123	42.835	6.703	0.343	0.114	40.731	6.882
SAV	0.5	0.123	44.18	7.398	0.469	0.117	43.12	7.885
GRS	0.269	0.109	49.379	5.63	0.26	0.106	46.408	5.919
PWET	0.428	0.184	33.155	9.433	0.393	0.188	32.717	8.813
CROP	0.518	0.129	43.597	4.824	0.502	0.131	41.569	5.446
URB	0.277	0.106	47.207	5.657	0.26	0.094	46.5	5.706
CP/NAT	0.414	0.104	45.029	3.806	0.375	0.113	40.883	4.674
BAR	0.13	0.085	54.291	7.46	0.129	0.086	52.23	7.714